Lattice-gas model of chemisorption on metal surfaces[1)]

V. P. Zhdanov and K. I. Zamaraev

Institute of Catalysis, Siberian Branch of the Academy of Sciences of the USSR, Novosibirsk
Usp. Fiz. Nauk **149**, 635–670 (August 1986)

Information on lattice-gas models of the following surface phenomena is compiled in this review: phase diagrams; effect of adsorption on surface reconstruction; and, kinetics of elementary physical-chemical surface processes, including thermodesorption spectra, isothermal kinetics, and surface diffusion.

CONTENTS

1. INTRODUCTION

Surface science has now been intensively studied for many decades. This is attributable primarily to the fact that surface phenomena play an important role in different applications, ranging from microelectronics to multiton chemical production processes, most of which are based on heterogeneous catalysis. The study of surface phenomena is also of great interest from the standpoint of academic science, since it is a multidisciplinary field and there are many interesting unsolved problems here.

Surface science received a new impetus in the last 15 years, when single-crystal samples became comparatively widely accessible and diverse physical methods for studying surfaces were developed. The reproducibility and informativeness of the results obtained with single-crystal samples using modern physical methods for studying surfaces stimulated the development of the theory of surface phenomena.

In the case of chemisorption of atoms and simple molecules on close-packed faces of single crystals, the assumption of surface uniformity is often justified, i.e., it may be assumed that the adsorbed particles are distributed amongst equivalent unit cells. The nonideality of the adsorbed layer in this case is due to the lateral interactions between adsorbed particles. In statistical physics a system of interacting particles distributed among equivalent unit cells is called a lattice gas. It turns out that many phenomena occurring on the surfaces of solids (phase diagrams, kinetics of different processes) can be described on the basis of the lattice-gas model. This explains the increased interest shown in recent years in the two-dimensional lattice-gas model—one of the classical models of statistical physics.

Reviews of the application of the lattice-gas model to the description of phase diagrams of chemisorbed particles have already been published by now[1–5] (only the adsorption-induced reconstruction of the surface is omitted in these reviews). The discussion of phase diagrams in this review is therefore brief (we note, however, that we include an extensive bibliography; in particular, there are many references to papers which were not mentioned in Refs. 1–5).

A detailed analysis of papers in which the lattice-gas model is used to analyze the kinetics of surface phenomena has not yet been published. We shall therefore devote our primary attention precisely to kinetic phenomena.

Our goal is to describe as completely as possible the theoretical work. The formal theoretical results can be used to describe both chemical and physical adsorption. In illustrating the applications of the theory we present typical examples of the application of the model to the description of chemisorption on metals.[2)] This restriction is determined partly by our own interests and partly by the fact that at the present time it is precisely in this area that the most intensive experimental work is being done. We remind those readers who are not specializing in surface science that physically adsorbed particles are particles whose surface binding energy is less than 10 kcal/mole. The surface binding energy of chemisorbed particles, as a rule, exceeds 20 kcal/mole.

2. PHASE DIAGRAMS

Information about phase diagrams of adsorbed particles is of great interest from the general physical standpoint. Indeed, the detailed experimental and theoretical study of phase transitions (in particular, two-dimensional phase transitions) is one of the fundamental physical problems in which interest has remained undiminished for several de-

 0038-5670/86/080755-22$01.80

cades. In addition, phase diagrams are of great interest from the standpoint of the kinetics of surface processes. We call attention to three facts. First, at temperatures below the critical temperature, when ordered phases are formed on the surface, the kinetics of different surface phenomena obviously cannot be described by simple equations which do not take into account the ordering of the molecules. Second, information about phase diagrams enables the evaluation of the scale of the lateral interactions between adsorbed molecules; these interactions, as we shall see below, strongly influence the kinetics of different surface processes, even at temperatures above the critical temperature. Third, the problem of describing the kinetics of the phase transition itself is in itself important and interesting.

Phase diagrams of the adsorbed layer are studied experimentally primarily by means of low-energy electron diffraction.[8] The systematic employment of this method for the analysis of the arrangement of adsorbed particles began about 20 years ago. Since the extensive experimental information has accumulated in this field. In particular, information about more than 800 surface structures is collected in the review of Ref. 9. In most experimental studies the arrangement of the adsorbed particles is analyzed only for some specific coverages and in a comparatively narrow temperature range. The construction of the phase diagram of an adsorbed layer requires a detailed analysis of the arrangement of the molecules for all values of the coverage and over a wide temperature range. Such studies were first undertaken approximately ten years ago. From the standpoint of methodology the construction of the phase diagram is a complicated problem (the difficulties encountered here are analyzed in Refs. 3 and 8). Nevertheless, phase diagrams have now been obtained for many systems (Table I). The lattice-gas model is widely used for interpreting the experimental results. References to theoretical articles, devoted to the analysis of phase diagrams of specific systems, are also given in Table I.

The ordered arrangement of adsorbed particles on a surface can be commensurate as well as incommensurate with the arrangement of the surface atoms. In the first case, the lattice spacings of the adsorbed particles, are commensurate with the substrate spacing, while in the second case they are not. The qualitative properties of commensurate and incommensurate structures are entirely different.[8] In particular, the disordering of commensurate films occurs in a quite narrow temperature range, while for incommensurate films this process extends over a wide temperature range. The interpretation of these data is based on the qualitative difference between the vibrational spectra of the adsorbed particles. In commensurate structures the adsorbed particles usually occupy definite unit cells. The vibrational spectrum of adsorbed particles in this case starts at a nonzero frequency, determined primarily by the form of the potential well in the unit cell. In a two-dimensional system with such a spectrum long-range order is possible at very low temperatures.

Incommensurate films are formed when the lateral interaction energy of the adsorbed particles is comparable to or greater than the activation barrier for diffusion along the surface. In this case the adsorbed particles can occupy sites which are not correlated with the relief of the substrate. In this connection the vibrational spectrum of an incommensurate film contains an acoustic branch which starts at zero frequency. In such a two-dimensional system true long-range order is impossible: fluctuations in the positions of the adsorbed particles increase logarithmically as a function of the distance from an arbitrarily selected origin.[10] The ordering in incommensurate films is sometimes called in the literature extended short-range (or quasi-ideal) order. Transitions from an incommensurate to a commensurate lattice can occur as the coverage is varied. The general theory of two-dimensional incommensurate structures is developed in Refs. 11 and 12 (see also Refs. 13–16).

We shall study primarily commensurate structures, since such structures are encountered most often in the case of chemisorption. The classification of two-dimensional phase transitions based on the symmetry in commensurate structures in accordance with Landau's rules[10] is given in Refs. 17–19.

Commensurate structures can be described with the help of the lattice-gas model. In this model the Hamiltonian which describes the adsorbed particles has the simple form

$$H=\frac{1}{2}\sum_{i\neq j}\varepsilon_{ij}n_in_j, \tag{2.1}$$

where ε_{ij} is the lateral interaction energy of particles occupying the ith and jth cells; n_i and n_j are the occupation

TABLE I. List of references in which the phase diagrams of chemisorbed particles were studied (T_c is the maximum temperature at which ordering is still possible).

System	T_c, K	Experiment	Theory	System	T_c, K	Experiment	Theory
H/Fe (110)	265	33	34, 35	H/W (001)	390	53	54–57
H/Ni (111)	275	45	38–40	O/W (110)	710	31, 72	31, 32, 72
N_2/Ni (110)	150	61		O/W (112)	900	58	58
O/Ni (111)	450	37, 46	16, 37	Na/W (110)	$\simeq$ 300	59	
O/Ni (001)	$>$ 800	47		Ba/W (110)	130	43	
H/Mo (001)	$>$ 250	48		Au/W (110)	$>$ 1100	62	
CO/Ru (001)	$>$ 400	49		CO/Pt (110)	$>$ 600	63	
H/Pd (001)	260	29	27, 28, 30	Na/Ru (001)	440	64	
O/Pd (110)	$>$ 800	50	51, 52				

numbers; and, the factor 1/2 comes from the fact that in the summation each interaction is taken into account twice.

The nature of the lateral interactions between adsorbed particles is discussed in Refs. 20 and 21. Van der Waals interaction, electrostatic dipole-dipole interaction, as well as interaction via the substrate (this interaction is often said to be indirect) are possible. The dipole-dipole interaction is the most significant interaction in the case of adsorption of strong electron donors and acceptors, such as, for example, the atoms of alkali and alkaline-earth elements or oxygen atoms. In the case of covalent chemisorption on metals the interaction via the substrate is often the strongest; this interaction has an oscillatory character: $\varepsilon(R) \sim \cos(2k_F R)/R^5$, where k_F is the Fermi momentum and R is the distance between the particles. In addition, the indirect interaction is not necessarily a pair interaction, i.e., the interaction of, for example, three particles does not necessarily equal the sum of the pair interactions between these particles. The Hamiltonian (2.1) includes only pair interactions. The nonpaired part of the lateral interactions can be taken into account to a first approximation by including in the Hamiltonian of the lattice-gas model the so-called three-body interactions, described by terms of the type $\varepsilon_t n_i n_{i+1} n_{i+2}$. Sometimes it is apparently necessary to take into account interactions of higher order also, but in practical calculations such interactions are usually ignored. The general properties of lateral interactions between particles adsorbed on metals have now been studied comparatively completely. In some papers[22,23] attempts were made to calculate the magnitudes of the interactions for specific systems. On the whole, however, reliable *a priori* calculations of the magnitudes of the lateral interactions are a task for the future. At the present time the lateral interactions appearing in the Hamiltonian (2.1) must be regarded as empirical parameters.

When the occupation numbers n_i are replaced by $(1 - n_i)$ the coverage θ is replaced by $1 - \theta$. If the interaction between the particles is a pair interaction, then for all practical purposes this transformation leaves the Hamiltonian (2.1) unchanged. A number of general properties of the lattice-gas model with pair interactions follow from here. The most important property is the symmetry of the phase diagram relative to the coverage $\theta = 1/2$. It has been established experimentally in many studies that full symmetry of the properties of the adsorbed layer relative to the coverage $\theta = 1/2$ often does not occur, which is an additional argument for introducing nonpair interactions into the lattice-gas model. When such interactions are included there is no symmetry in the model relative to the coverage $\theta = 1/2$.

The thermodynamic properties of the adsorbed layer, in particular, the phase diagram, can be determined by calculating the grand partition function for the adsorbed particles. The difficulties involved in the exact solution of this problem are well known. With the exception of a few particular cases[24] this problem has to be solved approximately. Existing approximate methods for solving the problem can be conditionally divided into the following groups: the mean-field approximation, the cluster approximations (quasichemical approximation, Bethe-Peierls approximation, etc.), the series expansion method, renormalization-group methods, and finally the Monte Carlo method. The advantages and disadvantages of approximate methods have been discussed repeatedly,[1,24,25] so that we will not dwell on this question.

We proceed now to the description of phase diagrams for different types of lattices. The simplest diagrams occur for square lattices. We shall first study the case of lateral interactions between nearest neighbors only. In this case, as is well known, some analytical results have been obtained. If the adsorbed particles attract one another (the lateral-interaction energy ε_1 is negative), then a "surface gas—surface liquid" first-order phase transition is possible. The critical temperature T_c for such a phase transition is determined by the well-known Onsager formula:

$$\left|\operatorname{sh}\frac{\varepsilon_1}{2kT_c}\right| = 1, \quad kT_c = 0.567\,|\varepsilon_1|. \tag{2.2}$$

Onsager's solution gives the following expression for the density (scaled to one unit cell) of the surface liquid θ_+ and of the surface gas θ_-:

$$\theta_\pm = \frac{1}{2}\left\{1 \pm \left[1 - \left(\operatorname{sh}\frac{\varepsilon_1}{2kT}\right)^{-4}\right]^{1/8}\right\}.$$

This equation determines the phase diagram of the system (Fig. 1a).

Phase diagrams of the adsorbed layer can be constructed in different coordinates. The "temperature—coverage" coordinates are most convenient and informative, and are most widely used. The diagram shown in Fig. 1a as well as

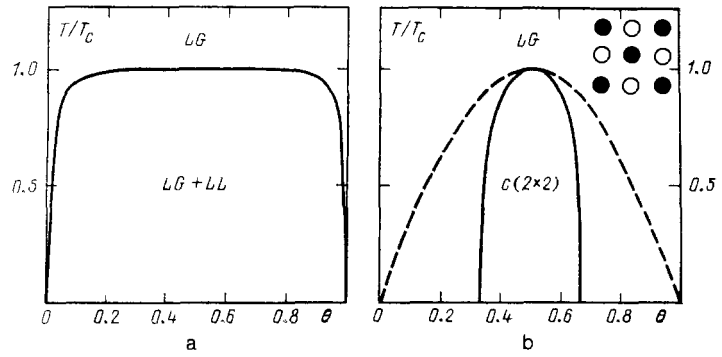

FIG. 1. Phase diagrams for particles arranged on a square lattice, taking into account the lateral interactions between nearest neighbors only. a) Attraction. b) Repulsion (the solid line shows the calculation by the Monte Carlo method,[26] the broken line corresponds to the mean-field approximation). *LG* denotes lattice gas, *LL* denotes lattice liquid, and T_c is the critical temperature. The arrangement of the particles corresponding to a c(2×2) structure is shown in the upper right-hand corner of Fig. 1b; the dark and light circles denote occupied and unoccupied cells.

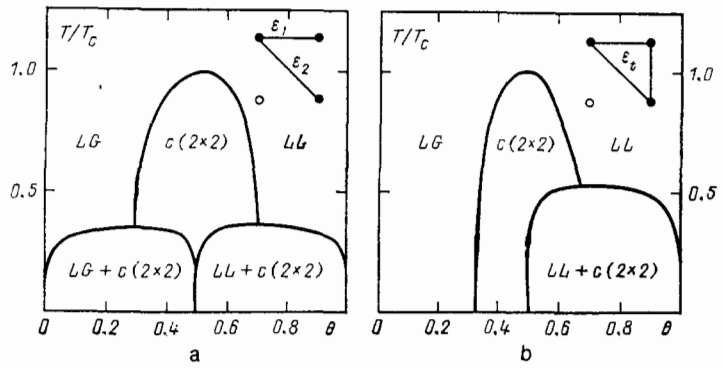

FIG. 2. Phase diagrams for particles arranged on a square lattice in the case of repulsion ($\varepsilon_1 > 0$) between nearest neighbors. a) Calculation of Ref. 28 for $\varepsilon_2/\varepsilon_1 = -0.5, \varepsilon_t = 0$. b) Calculation of Ref. 27 taking into account three-body interactions, $\varepsilon_t > 0$. The lateral interactions between particles are shown in the upper right-hand corners; the dark and light circles denote occupied and unoccupied cells.

subsequent diagrams are constructed precisely in these coordinates. We recall that the solid lines in the phase diagrams separate regions of temperatures and coverages corresponding to different phases (the different phases are characterized by the different symmetry of the arrangement of the molecules), or they separate one-phase regions from regions in which different phases coexist. In the case of the coexistence of different phases (for example, the region $LG + LL$ in Fig. 1a) the relative fraction of adsorbed molecules in one or the other phase is determined by the well-known "lever" rule.

The phase diagram shown in Fig. 1a is of interest for describing physically adsorbed particles. In the case of chemisorption the lateral interaction between neighboring particles is, as a rule, positive. In this case an "order—disorder" second-order phase transition occurs in the adsorbed layer. The lattice-gas model with repulsive interactions between neighboring particles corresponds, within the framework of the Ising model, to an antiferromagnetic substance. There is no spontaneous magnetization of the antiferromagnetic material in the absence of a field. In the language of the lattice-gas model this means that Onsager's solution in the absence of a field describes the characteristics of the adsorbed layer with a coverage of $\theta = 1/2$ only. In particular, the critical temperature with this coverage is determined as before by the formula (2.2), and the order parameter, equal to the difference of the average coverages of the two sublattices, is given by $\varphi = \{1 - [\mathrm{sh}(\varepsilon_1/2kT)]^{-4}\}^{1/8}$. The complete phase diagram (i.e., the dependence of the critical temperature on the coverage for all values of the coverage) for a square lattice with repulsive interaction between nearest neighbors (Fig. 1b) was first calculated[26] by the Monte Carlo method. It is evident that the ordered phase corresponds to a narrow coverage range near $\theta = 1/2$. Figure 1b also shows the diagram obtained in the mean-field approximation. This approximation substantially overestimates the region corresponding to the ordered phase. We recall that the mean-field approximation also overestimates by approximately a factor of two the critical temperature, giving at $\theta = 1/2 kT_c = \varepsilon_1$ instead of $kT_c = 0.567\varepsilon_1$.

The phase diagram for a square lattice, taking into account repulsion between nearest neighbors ($\varepsilon_1 > 0$) and attraction between next-to-nearest neighbors ($\varepsilon_2 < 0$), is shown in Fig. 2a. This diagram is a unique combination of the diagrams shown in Fig. 1. Taking into account the three-body interaction gives an asymmetry in the diagram relative to the coverage $\theta = 1/2$ (Fig. 2b).

An example of a real phase diagram for a square lattice is the diagram of the H/Pd(001) system shown in Fig. 3. In the experiment the ordered region was slightly shifted toward low coverage, and it was also broadened. This diagram is analyzed in Refs. 27, 28, and 30. The asymmetry of the diagram relative to the coverage $\theta = 1/2$ was explained by taking into account the three-body interaction. The broadening of the ordered region was not reproduced. The experimentally observed broadening is apparently attributable to the nonuniformity of the surface.[30] In addition, the broadening could be caused, in part, by the method used to determine the temperature of the phase transition. In the experiment of Ref. 29 the phase-transition temperature was taken as the

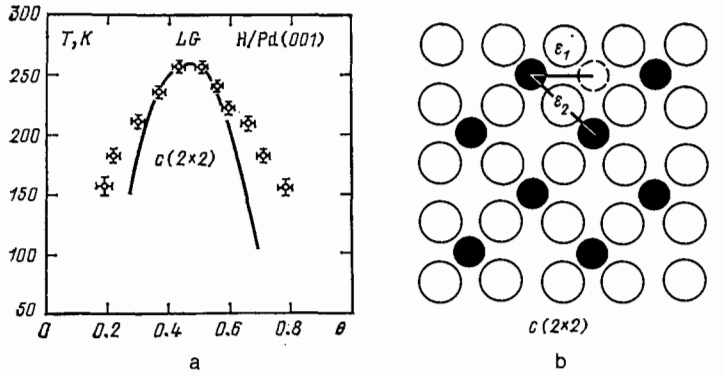

FIG. 3. a) Phase diagram of the system H/Pd (001); the symbols indicate the experimental data,[29] the solid line shows the theoretical calculation.[30] b) Assumed arrangement of particles on the surface corresponding to the c(2×2) structure; the dark circles are the hydrogen atoms and the light circles are palladium atoms.

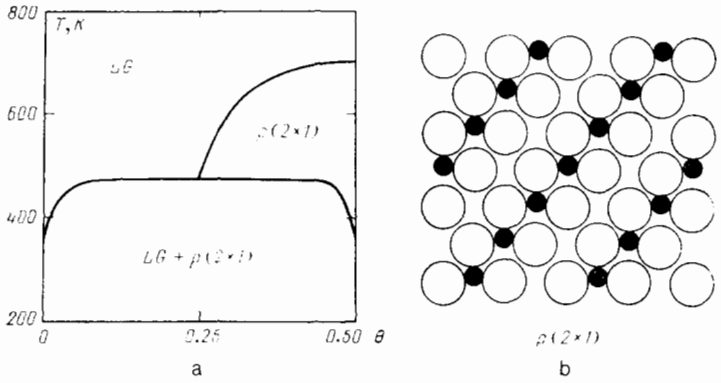

FIG. 4. a) Phase diagram of the system O/W (110).[31] b) Assumed arrangement of particles on the surface corresponding to the structure $p(2\times1)$; the dark circles indicate oxygen atoms and the light circles indicate tungsten atoms.

temperature corresponding to the inflection point on the graph of the intensity of elastic scattering of low-energy electrons as a function of the temperature. This method for determining the phase-transition temperature is not entirely correct (see the discussion in Ref. 30).

The next type of two-dimensional lattices is the rectangular centered lattice. An example of a real phase diagram for such a lattice is the diagram of the system O/W (110) shown in Fig. 4a. This diagram was analyzed theoretically in Refs. 31 and 32. When different types of lateral interactions are taken into account, separate sections of the diagram are reproduced. Another example of a phase diagram for adsorption on a rectangular centered lattice is the diagram of the system H/Fe (110) shown in Fig. 5. This diagram is discussed in Refs. 34 and 35. The best agreement with experiment is obtained (Fig. 6a) for the following values of the lateral interaction energies: $\varepsilon_1 = 0.3$, $\varepsilon_2 = 1.9$, $\varepsilon_3 = 0.5$, $\varepsilon_4 = -0.8$ kcal/mole.

The phase diagrams for particles located at the vertices of a rectangular lattice (or, what is the same thing, at the centers of the cells in a hexagonal lattice), are studied in Refs. 1 and 36; a list of previously published references on this subject is also given there.

The diagram constructed in Ref. 36 taking into account the lateral interactions ε_1 and ε_2 is shown in Fig. 7. An interesting feature of this phase diagram is the degeneracy (mixture) of ordered phases for coverages $\theta \approx 1/2$.

The phase diagrams for particles occupying the vertices of a hexagonal lattice are calculated in Refs. 16 and 37–40. Taking into account a limited number of lateral interactions enabled describing on a semiquantitative level the diagrams of the systems O/Ni (111)[16,37] and H/Ni (111).[38–40]

The results of systematic theoretical calculations and typical experimental data on phase diagrams of chemisorbed particles were presented above. Extensive experimental data are given in the original papers cited in Table I.

The values of the critical indices, characterizing the behavior of different thermodynamic quantities near the critical point, are of special interest for the general theory of phase transitions.[25] Experimental studies of critical indices in the case of phase transitions in an adsorbed layer are just beginning. The critical indices for the following structures have now been determined: p(2×2) – O/Ni (111),[41] p(2×1) – and p(2×2) – H/W (110),[42] p(3×2) – Ba/W (110),[43] p(2×1) – O/W (112).[44] Not all the results obtained are in agreement with the theory (the classification of critical indices according to symmetry is given in the reviews of Refs. 2 and 19 for two-dimensional phase transitions).

Aside from the calculation of phase diagrams, in recent years appreciable attention has been devoted to the study (primarily by the Monte Carlo method) of the kinetics of phase transitions.[73,74] When the temperature is lowered sharply, in the case of phase transitions of the order-disorder type, domain growth and relaxation of the energy of the system to a new equilibrium value obey the laws $R(t) \sim t^x$ and $E(t) - E(\infty) \sim t^y$. In the case when there are two thermodynamically equivalent methods for realizing an ordered structure ($p = 2$), $x = y = 1/2$.[73–75] If, on the other hand,

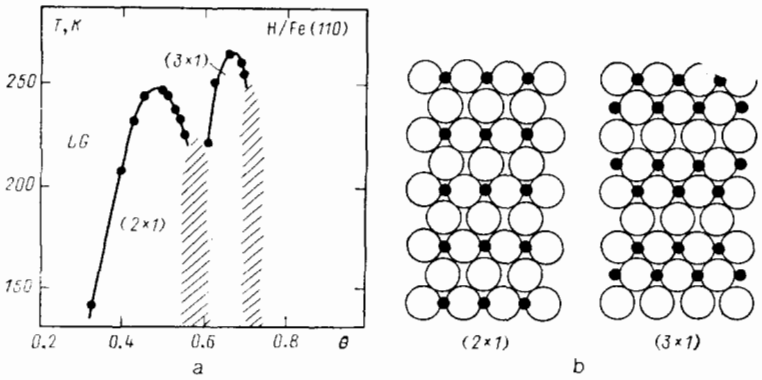

FIG. 5. a) Phase diagram for the system H/Fe (110)[33]; the shaded regions correspond to incommensurate structures. b) Proposed arrangement of particles on the surface corresponding to (2×1) and (3×1) structures; the dark circles denote hydrogen atoms and the light circles denote iron atoms.

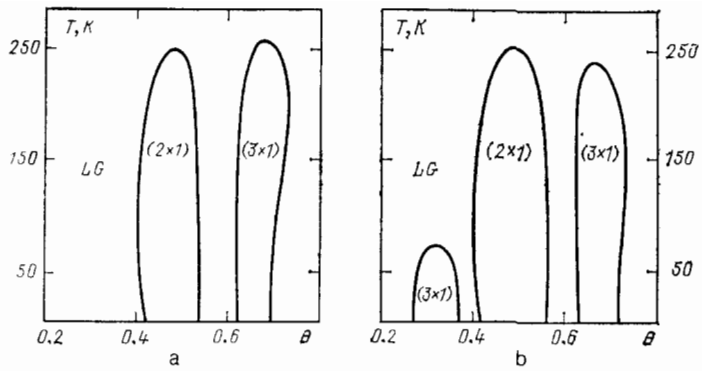

FIG. 6. Phase diagrams for a rectangular centered lattice with different types of lateral interactions, calculated[34] in order to reproduce the phase diagram of the system H/Fe (110).

the structure is multiply degenerate ($p > 2$), then the relaxation to equilibrium can be slower. For example, in the case of repulsive interactions $\varepsilon_1 = \varepsilon_2 > 0$ on a square lattice for coverages $\theta \approx 1/2$ a (2×1) four-fold degenerate structure is realized.[73]

In this case ordering occurs by the diffusion mechanism with the indices $x = y \approx 1/3$.[73]

Let us summarize. Extensive experimental data on surface phase transitions have now been accumulated. Real phase diagrams assume diverse forms, ranging from comparatively simple diagrams, such as, for example, the phase diagrams of the systems H/Pd (001)[29] and H/Ni (111),[45] up to very complicated diagrams, such as, for example, in the case of the system Na/Ru (001).[64] The phase-transition temperatures, as a rule, range from 300 K to 700 K (Table I). Such temperatures correspond to lateral nearest-neighbor interaction energies of 1 to 3 kcal/mole. Appreciable attention has also been directed toward theoretical calculations of the phase diagrams of the adsorbed layer. Based on the accumulated experience it may be concluded that phase diagrams calculated on the basis of the lattice-gas model, taking into account a small number of lateral interactions, reproduce the experimental results qualitatively and sometimes even quantitatively.

Further development of the theory in this field will apparently be directed toward the construction of a more detailed classification of the phase diagrams as a function of the type of lattice and type of lateral interactions.

3. EFFECT OF ADSORPTION ON SURFACE *RECONSTRUCTION*

The surface of many metals is rearranged under absorption. There are two large groups of metals.

a) Metals whose clean surface is reconstructed, i.e., the symmetry of the arrangement of the atoms on the surface differs from that of the atoms in the volume of the crystal. Under the action of adsorption the surface of the metal is rearranged in such a way that the arrangement of the atoms on the surface reverts to the spacing characteristic for the volume of the metal. Such systems include the (110) and (100) faces of the heavy metals Pt, Ir, or Au. In particular, the reconstruction of the Pt (100) surface accompanying adsorption of CO, NO, and hydrogen was studied in detail in Refs. 65 and 66. It was shown that absorption-induced reconstruction can be regarded as a first-order phase transition. This result is based on the fact that when even a small quantity of adsorbent is adsorbed patches of a new phase are formed on the surface. Hydrogen-induced reconstruction of the Ir (100) surface was studied in Ref. 60. In the case of both Pt and Ir, the atoms of the clean reconstructed (100) surface are arranged nearly hexagonally, and they form a structure of the (5×1) type. Adsorption stimulates the surface atoms to revert to the (1×1) structure characteristic for the volume of the metal.

b) Metals whose clean surface is not reconstructed, i.e., the symmetry of the arrangement of atoms on the surface

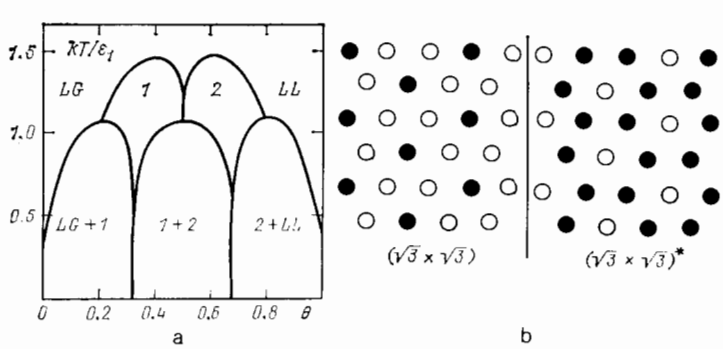

FIG. 7. a) Phase diagram for particles arranged at the vertices of a triangular lattice, calculated[36] taking into account the lateral interactions $\varepsilon_1 > 0$ and $\varepsilon_2 = -\varepsilon_1$. b) Arrangement of particles corresponding to the structures $(\sqrt{3}\times\sqrt{3})$ and $(\sqrt{3}\times\sqrt{3})^*$. The dark and light circles denote occupied and unoccupied cells.

corresponds to that of the atoms in the volume of the crystal. Adsorption changes the symmetry of the arrangement of the atoms on the surface. This group includes primarily the (110) faces of face-centered and (100) and (110) faces of body-centered metals. The adsorption-induced reconstruction of the type under discussion has been studied for the following examples (references are given in Ref. 65): O/Cu (110), H/Ni (110), O/Ni (110), N/Mo (100), H/Pd (110), H/W (100), N/W (100). Of these systems the hydrogen-induced reconstruction of the W (100) surface has been studied in greatest detail.[63] It was established that at temperatures above room temperature the arrangement of the atoms on a clean W (100) surface corresponds to the arrangement in the volume. As the temperature is lowered the atoms on the surface are displaced, forming a c(2×2) structure. This second-order phase transition is reversible. Adsorption of a small quantity of hydrogen raises the phase-transition temperature. When a significant amount of hydrogen is adsorbed, the structure of the surface layer becomes incommensurate with the arrangement of atoms in the volume of the single crystal.

A semiphenomenological model of the effect of adsorption of a small quantity of hydrogen on the reconstruction of the W (001) surface is proposed in Ref. 54. This is the first model of the complicated phenomenon of adsorption-induced surface reconstruction. For this reason, we shall give a brief exposition of the basic ideas of Ref. 54.

The Hamiltonian describing the interaction of adsorbed atoms with one another and the interaction of adsorbed atoms with atoms in the lattice has the form

$$H_{ad}=\frac{1}{2}\sum_{i\neq j}\varepsilon_{ij}n_in_j+\sum_{i,\,l}n_iU(R_l^0+u_l-R_i), \qquad (3.1)$$

where ε_{ij} is the energy of lateral interactions between adsorbed hydrogen atoms, n_i is the occupation number of the surface cells for hydrogen atoms. $U(R)$ is the interaction potential between the hydrogen and tungsten atoms, R_i is the coordinate of a hydrogen atom, R_l^0 is the coordinate of the tungsten atom before reconstruction, and u_l is the change in the coordinates of the tungsten atom accompanying reconstruction. The Hamiltonian (3.1) differs from the standard lattice-gas Hamiltonian in that it allows for the possibility of displacement of tungsten atoms.

The experimentally observed c(2×2) structure of the reconstructed surface corresponds to displacements of tungsten atoms in the directions $\mathbf{K}=(\pi/a)(1,1)$ or $\mathbf{K}'=(\pi/a)(1,-1)$, where a is the lattice spacing (see Fig. 8). If attention is confined to displacements in the direction $\mathbf{K}$, the displacement vector can be represented in the form

$$u_l=a\varphi\mathbf{K}\cos(\mathbf{K}\mathbf{R}_l^0), \qquad (3.2)$$

where φ is the order parameter. The hydrogen atoms on the surface occupy bridging positions. Since there is an interaction between the hydrogen and tungsten atoms which depends on the mutual arrangement of these atoms, the displacement (3.2) of tungsten atoms changes the average occupation numbers of the cells of the lattice. This change evidently has the form

$$\langle n_i\rangle=\frac{\theta}{2}+m\sin(\mathbf{K}\mathbf{R}_i), \qquad (3.3)$$

where m is a free parameter and θ is the coverage of the surface, defined so that $\theta=1$ corresponds to one hydrogen atom per tungsten atom on the surface. The change in the occupation numbers (3.3) does not cause the average occupation numbers of the two interpenetrating sublattices, shown in Fig. 8 by the small circles and squares, to become different. Nevertheless, the average occupation numbers of the two sublattices can become different as a result of an order-disorder phase transition in the adsorbed layer. Analysis[54] shows, however, that a phase transition of this type and the modulation (3.3) of the average occupation numbers are mutually exclusive. We shall therefore ignore here the possibility that the average occupation numbers of the two interpenetrating lattices are different.

In the mean-field approximation the free energy corresponding to the Hamiltonian (3.1) and the lateral interactions shown in Fig. 8 has the form

$$\begin{aligned}\frac{F_{ad}}{N_s}&=-2\lambda m\varphi+4\varepsilon_2m^2\\&+kT\left[\left(\frac{\theta}{2}+m\right)\ln\left(\frac{\theta}{2}+m\right)\right.\\&\left.+\left(1-\frac{\theta}{2}-m\right)\ln\left(1-\frac{\theta}{2}-m\right)\right]\\&+kT\left[\left(\frac{\theta}{2}-m\right)\ln\left(\frac{\theta}{2}-m\right)\right.\\&\left.+\left(1-\frac{\theta}{2}+m\right)\ln\left(1-\frac{\theta}{2}+m\right)\right],\end{aligned} \qquad (3.4)$$

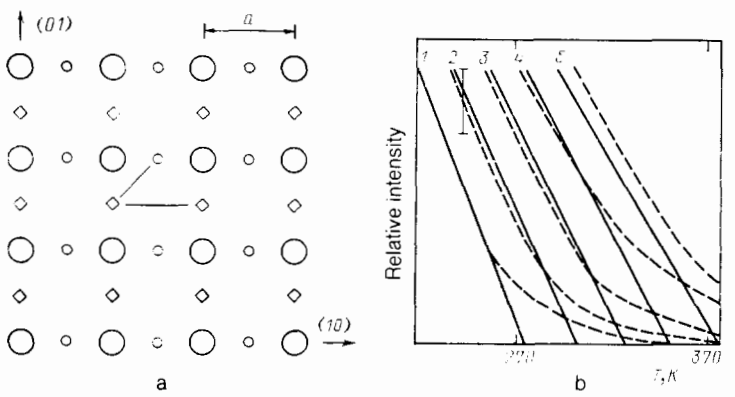

FIG. 8. a) Diagram showing the arrangement of particles on the W (001) surface; the large circles denote tungsten atoms and the small circles and diamonds denote the locations at which hydrogen atoms are adsorbed. b) Relative intensity of additional (1/2, 1/2) LEED spots; the broken lines correspond to experiment[53] and the solid lines correspond to calculations[54] based on Eqs. (3.5); the graphs 1–5 were constructed for coverages $\theta=0$, 0.036, 0.072, 0.107, and 0.143, respectively.

where N_s is the number of tungsten atoms on the surface and λ is a coefficient, which is proportional to the Fourier component of the gradient of the potential $U(R)$ and describes the interaction of hydrogen and tungsten atoms. We did not include in the free energy (3.4) a term proportional to the lateral interaction energy ε_1, since this term does not depend on the parameters m and φ and therefore does not affect the reconstruction. The free energy (3.4) is the free energy of adsorbed particles. To describe the free energy of the tungsten surface it is necessary to know the microscopic nature of the phase transition on a clean surface. Possible factors responsible for the reconstruction of a clean surface are discussed in Refs. 55, 76, and 77, but this problem has not yet been solved completely. For this reason, in Ref. 54 Landau's phenomenological expression was used to describe the free energy of the tungsten surface itself:

$$\frac{F_s}{N_s} = r(T - T_s)\varphi^2 + v\varphi^4,$$

where T_s is the temperature of the phase transition of the clean surface, and r and v are constants which, to a first approximation, are temperature independent. Minimization of the total free energy $F = F_{ad} + F_s$ with respect to the parameters φ and m gives the following equation for determining these parameters:

$$\left.\begin{aligned} r(T - T_s)\varphi + 2v\varphi^3 - \lambda m = 0, \\ -\lambda\varphi + 4\varepsilon_2 m + \frac{kT}{2}\ln\frac{(\theta+2m)(2-\theta+2m)}{(\theta-2m)(2-\theta-2m)} = 0. \end{aligned}\right\} \quad (3.5)$$

For low coverage Eqs. (3.5) imply a linear dependence of the phase-transition temperature on the coverage

$$T_c(\theta) = T_s + \frac{\lambda^2\theta}{2rkT_s}.$$

The physical reason for the growth in the critical temperature is the ordering of the adsorbed layer accompanying reconstruction. The increase in the free energy (and, as a consequence, the increase in T_c) accompanying ordering is all the smaller the higher the coverage.

The reconstruction of the W (001) surface is recorded experimentally by observing the additional (1/2, 1/2) spots in the elastic scattering of low-energy electrons. If the narrow temperature range near $T_c(\theta)$—the temperature of the phase transition—is excluded from the analysis, then the intensity of the additional spots is proportional to φ^2—the square of the order parameter. According to Eqs. (3.5) the value of the order parameter depends on the temperature, the coverage, and the five parameters T_s, r, v, ε^2 and λ. The first three parameters were determined in Ref. 54 from data on the reconstruction of the clean surface, the parameter ε_2 was determined from the thermodesorption data, and the fifth parameter λ was chosen so as to obtain the best description of the experimental results from LEED. The experimental and theoretical results are compared in Fig. 8. With the exception of the narrow temperature range $|T - T_c(\theta)|/T_c(\theta) < 0.05$, near the phase-transition temperature the experimental and theoretical results are in good agreement with one another. In the immediate vicinity of $T_c(\theta)$—the phase-transition temperature, both long- and short-range order in the arrangement of the tungsten atoms on the surface make a significant contribution to the intensity of the elastic scattering of low-energy electrons. In the mean-field approximation short-range order is actually excluded from the analysis. For this reason, disagreement between theory and experiment in this temperature range is not unexpected.

Thus it turns out that the effect of adsorption on reconstruction can be described on the basis of a semiphenomenological model.[54] This model reproduces the experimental results on the adsorption of a small quantity of hydrogen on the W (001) surface. It is further developed in Refs. 55–57, and in particular the effect of adsorption of a significant quantity of hydrogen on the reconstruction of the W (001) surface is studied in Ref. 57. In this case the structure of the surface layer becomes incompensurate with the arrangement of tungsten atoms in the volume of the single crystal.

A simple model of adsorption-induced surface reconstruction as a first-order phase transition is proposed in Refs. 67 and 68. This model describes qualitatively the reconstruction of the type described above for the Pt (100) surface accompanying adsorption of CO, NO, and hydrogen. It is presumed that the atoms on the surface can occupy two positions, I and II. On a clean surface the position I is stable, while the position II is metastable. The adsorbed particles can be described by a lattice-gas model. The free energy of the system (per unit surface area) is calculated in the mean-field approximation:

$$\left.\begin{aligned} F &= F_{ad} + F_s + F_{int}, \\ \frac{F_{ad}}{N_s} &= -E_{ad} + \frac{1}{2}z\varepsilon_1\theta^2 + T[\theta\ln\theta + (1-\theta)\ln(1-\theta)], \\ \frac{F_s}{N_s} &= \Delta E\cdot\varkappa + T[\varkappa\ln\varkappa + (1-\varkappa)\ln(1-\varkappa)], \\ \frac{F_{int}}{N_s} &= -z\alpha\theta\varkappa, \end{aligned}\right\} \quad (3.6)$$

where F_{ad} is the free energy of the adsorbed particles, F_s is the free energy of the atoms on the surface, F_{int} is the interaction energy of the adsorbed particles and the surface atoms (this interaction stabilizes the metastable phase), N_s is the number of atoms of the metal per unit area of the surface, E_{ad} is the adsorption energy, $\theta = N/N_s$ is the coverage of the surface by adsorbed particles, N is the number of adsorbed particles per unit surface area, z is the number of neighboring cells, ε_1 is the lateral interaction energy of two adsorbed nearest-neighbors, ΔE is the difference between the energies in positions II and I in the case of a clean surface, $\varkappa$ is the relative fraction of surface atoms occupying II positions, and α is a parameter characterizing the interaction energy of adsorbed particles and surface atoms.

The following expression can be obtained[67,68] from Eqs. (3.6) for the chemical potential of the adsorbed particles:

$$\exp\frac{\mu + E_{ad}}{T} = \frac{\theta}{1-\theta}\exp\left[\frac{z\varepsilon_1\theta}{T} - \frac{z\alpha}{T\{1+\exp[(\Delta E - z\alpha\theta)/T]\}}\right]. \quad (3.7)$$

This equation determines the phase diagram of the system. At temperatures below the critical temperature, $T < T_c$, the right side of Eq. (3.7) is a nonmonotonic function of the coverage. Thus phase separation occurs for $T < T_c$. The physical reason for the phase transition is that the metastable phase is stabilized by the adsorbed particles.

Equation (3.7) can also be used to construct adsorption isotherms or isobars. For example, in the case of monomolecular adsorption the chemical potential of the adsorbed particles equals the chemical potential of the particles in the gas phase. The chemical potential of the gas phase is given, as is well known, by the expression

$$\mu = T \ln \frac{N_{gas}}{Z_{gas}}, \tag{3.8}$$

where N_{gas} is the density of molecules and Z_{gas} is the partition function. Equations (3.7) and (3.8) determine the adsorption isotherms and isobars.

The possible effect of adsorption-induced reconstruction on the kinetics of surface processes was discussed in Ref. 68. The simplest consequence of reconstruction (as a first-order phase transition) could be sharp changes in the surface coverage by adsorbed particles as the pressure or temperature varies in adsorption-desorption or adsorption-reaction equilibria. A sharp change in the coverage is accompanied by a transition of the surface from one phase into another. The first-order phase transition proceeds via the formation and growth of nuclei of the new phase. In the case of reconstruction the kinetics of the phase transition can be slow, since the change in the positions of the surface atoms is an activated process. For example, the energy of activation of the transition of an almost clean Pt (100) surface from a (1×1) structure into a (5×1) structure equals approximately 20 kcal/mole, while the characteristic transition time at a temperature of 413 K equals several minutes.[66] Hysteresis phenomena in transitional states could be a consequence of slow restructuring. Hysteresis of this type was apparently observed to accompany the adsorption of CO[65] and oxidation of hydrogen.[69]

Interesting experimental results were obtained in Refs. 70 and 71 in the study of the oxidation of CO on a Pt (100) surface. At temperatures $T\approx500$ K and pressures $P_{O_2}\approx10P_{CO}\approx10^{-4}$ torr the reaction rate oscillated with a period of several minutes. Surface reconstruction was observed during the oscillations. Unfortunately, at the present time it is difficult to construct a model which would adequately describe such oscillations and would enable clarifying the role of adsorption-induced surface reconstruction in them.

The study of the extent to which induced surface reconstruction, as a second-order phase transition, affects the kinetics of surface processes is only beginning. In particular, the effect of induced reconstruction of the W (100) surface on the thermodesorption spectra of hydrogen has been studied experimentally[161] and theoretically.[162]

4. GENERAL APPROACH TO THE DESCRIPTION OF THE KINETICS OF ADSORPTION, DESORPTION, AND CHEMICAL REACTIONS ON A SURFACE

The study of the kinetics of adsorption, desorption, and chemical reactions on a surface is of great practical interest. This is attributable to the fact that many important chemical reactions occur in the gas phase, or with a low rate, or with a low yield of useful products. The realization of the reaction on the surface of a catalyst with the required properties makes it possible to accelerate the reaction and to increase the yield of useful products. At the present time heterogeneous catalysis is the cornerstone of the chemical industry. Optimization of catalytic reactions is impossible without detailed data on their kinetics.

The simplest model for describing the kinetics of the elementary stages of a chemical reaction on a surface is the model of an ideal adsorbed layer (lattice-gas without lateral interactions). On the basis of this model the kinetics of elementary processes is described by simple power-law equations (the monomolecular desorption rate is proportional to the coverage of the surface by adsorbed particles, the rate of bimolecular reactions between adsorbed molecules is proportional to the product of their coverages, etc.). The model of an ideal adsorbed layer is attractive because of its simplicity. For this reason, it is widely used for qualitative analysis of surface phenomena. A real adsorption layer, as a rule, is substantially nonideal, owing to the nonuniformity of the surface, lateral interactions between adsorbed particles, or the different nature of adsorption-induced restructurings of the surface.

The simplest method for describing a nonuniform surface is based on the idea that the surface consists of a collection of ideal sections. The nonideality of the kinetics in this case is obtained by averaging the ideal kinetics over some parameters, for example, the surface binding energy of adsorbed particles. This method is formal. The construction of a more detailed theory is precluded by the fact that the structure of a nonuniform surface is often too complicated to be adequately described theoretically.

In the case of a uniform surface, i.e., a surface consisting of equivalent unit cells, the nonideality of the kinetics is determined by the lateral interactions between adsorbed particles. In this section we shall present the basic principles of the description of the kinetics of elementary processes on a uniform surface taking into account lateral interactions.

The calculation of the rate of an elementary surface process is a difficult problem, involving the description of both the dynamics of motion and the statistical characteristics of the adsorbed particles (for definiteness, we assume that they are molecules). To a first approximation the effect of the molecules surrounding a molecule or a pair of molecules entering directly into the elementary transformation reduces to a shift of the bottom of the potential well and the top of the potential barrier owing to the lateral interactions. In this approximation the dynamic and statistical parts of the problem are decoupled, and the dependence of the rate of the process on the surface coverage by the molecules is determined wholly by the statistical characteristics of the molecules. Analysis of the dynamics of the nuclei is necessary only for determining the absolute magnitude of the preexponential factor in the rate constant of the process. Here we are interested only in the statistical part of the problem. We refer readers who are interested in the dynamics of the motion of adsorbed particles to the reviews given in Refs. 78–80.

The effect of lateral interactions on the rate of elementary surface processes has been discussed in many arti-

cles.[81-101] In all of them the decoupling of the dynamic and statistical parts of the problem, described above, was employed. Nevertheless Refs. 81–101 differ substantially from one another with respect to the formalism employed as well as the level of generality, rigor, and clarity of exposition. The most general results were obtained, in our opinion, in Ref. 93; different approaches are discussed and compared, and in particular it is demonstrated that some of them are equivalent.

The general formulas for describing the rates of elementary processes in the lattice-gas model have a simple form. The rate of an elementary process, as usual, is expressed in terms of the energy difference between the bottom of the potential well and the top of the potential barrier for the motion of the molecules. We shall call the state of the system near the top of the potential barrier, as is customarily done in chemistry, an activated complex. As an example, we present an expression for the rate of the bimolecular reaction $A_s + B_s \to (AB)_{gas}$ between adsorbed molecules:

$$\frac{d\theta_A}{dt} = \frac{d\theta_B}{dt} = -R_r(\theta_A, \theta_B), \tag{4.1}$$

$$R_r = \nu \sum_i P_{AB,i} \exp\left[-\frac{1}{kT}(E_a(0) + \Delta\varepsilon_i)\right], \tag{4.2}$$

where R_r is the reaction rate, $P_{AB,i}$ is the probability that the pair AB of neighboring adsorbed particles has an environment denoted by the index i, $E_a(0)$ is the activation energy of the reaction in the limit of low coverage, $\Delta\varepsilon_i = \varepsilon_i^* - \varepsilon_i$, ε_i and ε_i^* are the lateral interaction energies between the pair AB and the surrounding particles and between the activated complex A*B* and the same environment,[3)] and ν is a preexponential factor whose value is of the order of the vibrational frequency of the atoms in the molecules $\nu \approx 10^{13} - 10^{14}\ s^{-1}$.

The formulas (4.2) have a simple physical interpretation. The particles surrounding the reacting pair change the magnitude of the activation energy of an elementary transformation act. Summation of all possible configurations of the surrounding particles gives the observed value of the rate of the process.

The conditions of applicability of formulas of the type (4.1)–(4.2) are actually the same as those of the lattice-gas model for adsorbed particles. The particles must occupy equivalent cells, and in addition an individual cell can contain only one particle. These conditions usually hold in the case of chemisorption on a uniform surface.

The algorithm for constructing general expressions of the type (4.1)–(4.2) for the rates of different processes is obvious. In particular, the expressions for the rates of the reverse processes have the same form. It is shown in Ref. 95 for the example of monomolecular adsorption and desorption that formulas of the type (4.1)–(4.2) correctly describe the thermodynamic equilibrium, i.e., for example, the fact that the rates of adsorption and desorption are equal implies that the chemical potentials of the molecules in the gas phase and in the adsorbed layer are equal.

Formulas of the type (4.1)–(4.2) are not so much a solution as a formulation of the problem of calculating the rate of an elementary process, since the main difficulty lies in calculating the probabilities appearing in these formulas.

The kinetics of real surface processes is usually studied at comparatively high temperatures, where there is no long-range order in the arrangement of the adsorbed molecules. In this temperature range the cluster method is the most suitable method for calculating the rates of elementary processes. As a rule, the practical calculations take into account the lateral interactions only between nearest neighbors and the quasichemical approximation or the Bethe-Peierls approximation is used. In particular, the quasichemical approximation has been used[93] to describe monomolecular adsorption and desorption, associative desorption, dissociative adsorption, bimolecular reactions between adsorbed molecules, and bimolecular reactions between adsorbed molecules and molecules from the gas phase.

In concluding this section we shall compare some results obtained in the quasichemical approximation[93] with the results of calculations performed by the Monte Carlo method.[91] The Monte Carlo method is still not used widely for describing the kinetics of elementary surface processes. Reference 91 is one of the few works on this subject. In Ref. 91, the process of associative desorption of nitrogen atoms in the presence of oxygen atoms on the surface is studied (the nitrogen and oxygen atoms on the surface of platinum-group metals are formed as a result of dissociative adsorption of NO molecules, and then under heating associative desorption of nitrogen primarily occurs). The dependence of the activation energy of desorption of nitrogen on the coverage of the surface by nitrogen and oxygen was calculated. The calculations were carried out for three sets of lateral interactions (Fig. 9). In the cases of Figs. 9a and b the results obtained by the two methods are in good agreement with one another. In the case of Fig. 9c there is strong disagreement. This disagreement is apparently caused by the fact that the magnitude of the following combination of lateral energies is very large: $|\varepsilon_{AA} + \varepsilon_{BB} - 2\varepsilon_{AB}| = 10\ kT$. In this case the

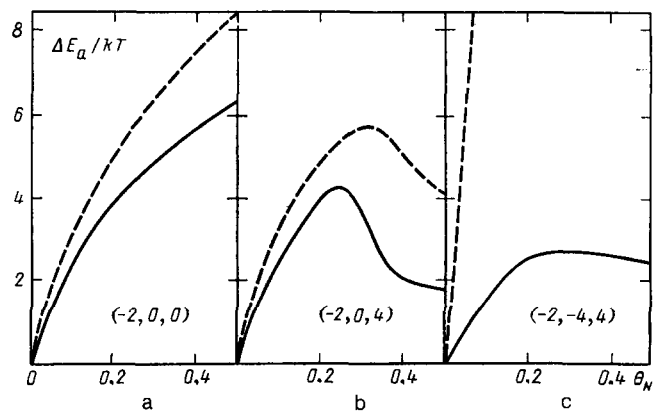

FIG. 9. Dependence of the quantity $\Delta E_a(\theta_N, \theta_0) = E_a(\theta_N, \theta_0) - E_a(0, \theta_0)$ on θ_N—the coverage of the surface by nitrogen atoms. The coverage of the surface by oxygen atoms is constant and equals $\theta_0 = 0.5$; $E_{ad}(\theta_N, \theta_0)$ is the activation energy for associative desorption of nitrogen atoms. The solid lines correspond to the calculation[91] by the Monte Carlo method and the broken lines correspond to the quasichemical approximation.[93] A combination of the type (−2, −4, 4) denotes $\varepsilon_{AA}/kT = -2$, $\varepsilon_{AB}/kT = -4$, $\varepsilon_{BB}/kT = 4$.

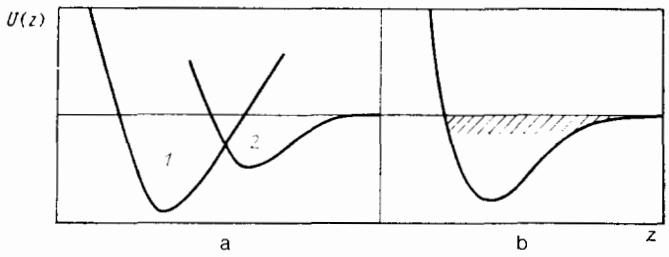

FIG. 10. The potential energy for the motion of a molecule as a whole in the direction away from the surface. z is the distance between the molecule and the surface. a) Diagram with a real preadsorption state; 1 and 2 denote the chemiadsorbed and preadsorbed states. b) No real preadsorbed state; the role of the preadsorbed state is played by a group of strongly excited vibrational states (shown by the hatch marks) of molecules as a whole in the adsorption potential.

quasichemical approximation is apparently not valid. In addition, it is not completely clear whether or not thermodynamic equilibrium is achieved in the layer with such a large value of the parameter $|\varepsilon_{AA} + \varepsilon_{BB} - 2\varepsilon_{AB}|/kT$, since the computing time required for reaching equilibrium increases very rapidly as the parameters ε_{AA}/kT, ε_{BB}/kT and $|\varepsilon_{AA} + \varepsilon_{BB} - 2\varepsilon_{AB}|/kT$ increase.

5. EFFECT OF PREADSORPTION STATES ON ADSORPTION AND DESORPTION KINETICS

In the derivation of formulas of the type (4.2) it was assumed that the unit cell on the surface can be occupied by only one adsorbed molecule, i.e., processes like hopping of a molecule from one cell into an occupied cell were excluded from the analysis. Such processes are possible, however, and they affect the dependence of the adsorption and desorption rates on the coverage. From the standpoint of formal kinetics it is convenient to describe processes in terms of the so-called preadsorption states. Preadsorption states above an occupied cell and above an unoccupied cell are distinguished. The preadsorption state of a molecule hopping into an occupied cell is the physically adsorped state above an occupied cell. The nature of the preadsorption state above a free cell is more complicated and not unique. On the one hand, a real preadsorption state, corresponding to the excitation of electrons in the adsorbate + solid system (Fig. 10a), may exist. On the other hand, a real preadsorption state may not exist, i.e., the particle-surface interaction potential can have the standard form of one well (Fig. 10b). In the latter case, the group of strongly excited vibrational states of a particle in the adsorption potential plays the role of the preadsorption state. Indeed, in such states an adsorbed particle can hop over to neighboring occupied as well as unoccupied cells. If the entire group of weakly excited vibrational states of a particle in the adsorption potential is characterized by one effective state, then from the standpoint of formal kinetics the situations with the real and the effective preadsorption state above an occupied cell are completely equivalent. It is usually difficult to determine unequivocally from the experimental data whether the preadsorption state above an unoccupied cell is real or effective. It should only be noted that the presence of a real preadsorption state is an additional obstacle for absorption. For this reason, other conditions remaining the same, the existence of such a state should lead to a reduction of the sticking coefficient, and therefore it may be expected that in this case, in the limit of low coverage, the sticking coefficient must be much less than unity. If this is not the case, then the picture without a real preadsorption state should apparently be given priority.

The formulas describing the effect of preadsorption states on the kinetics of monomolecular and associative desorption were first derived in classical papers[102] from a calculation of the probabilities of chains of different processes. The arrangement of molecules on the surface was regarded as random, i.e., lateral interactions between adsorbed molecules were ignored. Analogous results were obtained later in Refs. 103–107. The problem was solved by two methods: either the probability of the chains of different events was calculated or the method of kinetic equations was used. It was shown in Ref. 107 that these two approaches are equivalent. The method of kinetic equations, however, is formally simpler.

The kinetics of adsorption and desorption, taking into account both lateral interactions between adsorbed molecules and preadsorption states, was studied in Refs. 84, 85, and 93. The most general results for monomolecular adsorption and desorption were obtained in Ref. 93.[4)] It was shown that the ordering of the molecules in the adsorbed layer has virtually no effect on the sticking coefficient. The physical reason for this is that a molecule, wandering over preadsorption states above occupied cells, will ultimately encounter an empty cell and will be adsorbed onto it, irrespectively of whether or not the arrangement of adsorbed particles is ordered. The typical dependence of the sticking coefficient on the coverage in the case of monomolecular adsorption is shown in Fig. 11. For the example shown in Fig. 11, for high

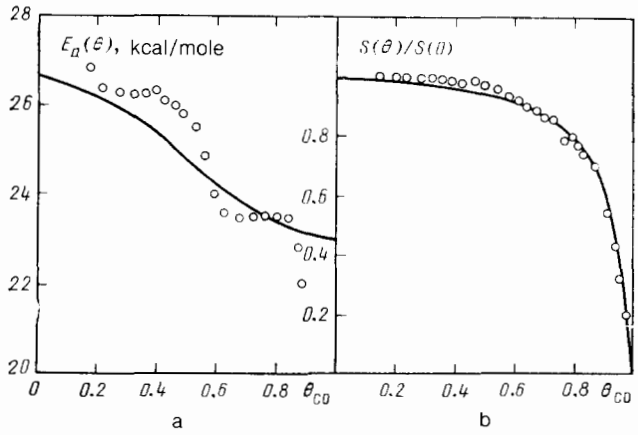

FIG. 11. Dependence of the desorption activation energy and the sticking coefficient (at 300 K) on the coverage for the system CO/Ni (111). The circles denote the experimental points,[108] and the solid line corresponds to the calculation of Ref. 93.

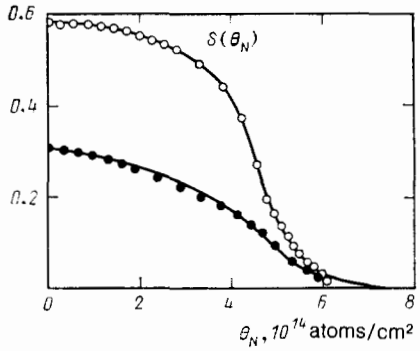

FIG. 12. Dependence of the sticking coefficient on the coverage for dissociative adsorption of N_2 on the W (001) surface.[84] The light and dark circles correspond to the experimental values at temperatures of 300 and 663 K; the solid lines show the calculation taking into account the preadsorbed states.

coverage a CO molecule, having collided with the surface and having occupied a preadsorption state, completes up to 10 hops along the surface before it is adsorbed or desorbed back into the gas phase.

The effect of preadsorption states on the monomolecular desorption rate reduces to premultiplication of the right side of expression (4.2) by the factor $S(\theta)/[S(0)(1-\theta)]$, where $S(\theta)$ is the sticking coefficient, calculated taking into account the preadsorption states.

Ordering of adsorbed molecules has a substantial effect on the kinetics of dissociative adsorption. For dissociative adsorption the molecule must hit in collisions with the surface a section of the surface consisting of two adjacent empty cells. As a result of repulsion between adsorbed particles the probability for finding two adjacent empty cells decreases rapidly as the coverage increases. This leads to a rapid drop in the sticking coefficient as the coverage increases. Preadsorption states have the effect of smoothing this effect for low coverages. As a result, in a narrow range of low coverage the sticking coefficient remains approximately constant, after which it decreases rapidly (see, for example, Fig. 12). Equations describing the effect of preadsorption states and ordering of molecules in the adsorbed layer on the kinetics of dissociative adsorption are analyzed in detail in Ref. 85.

6. EFFECT OF LATERAL INTERACTIONS BETWEEN ADSORBED PARTICLES ON THE PREEXPONENTIAL FACTOR IN THE DESORPTION RATE CONSTANT

The desorption rate constant is usually described by the phenomenological equation

$$k_d(\theta) = \nu(\theta)\, e^{-E_a(\theta)/kT} \qquad (6.1)$$

In accordance with the representation (6.1) the activation energy and the preexponential factor are determined by the relations

$$E_a(\theta) = kT^2 \frac{d}{dT} \ln k_d(\theta), \qquad (6.2)$$

$$\nu(\theta) = k_d(\theta)\, e^{E_a(\theta)/kT}. \qquad (6.3)$$

The preexponential factor calculated according to the formulas (6.2) and (6.3), generally speaking, differs from the preexponential factor appearing in formulas of the type (4.2), since the sum in expressions of the type (4.2) is not represented in the form of a simple exponential. In particular, the preexponential factor (6.3) can depend on the coverage.

In the last few years attempts have been made to measure accurately the dependence on the coverage of the activation energies and preexponential factors in the rate constants for the desorption of atoms and some simple molecules. The following systems are examples of systems which have been studied: CO/Ru (001),[109,110] CO/Ir (110),[111,112] CO/Ni (111),[108,113] NO/Pt (111),[114] Ba/W (001).[115] To determine the dependence of the parameters in the rate constant of the process on the coverage it is necessary to measure the rate of the process with a constant coverage over a comparatively wide range of temperatures. From the experimental viewpoint this is a difficult problem, since as the temperature is raised the coverage of the surface by adsorbed molecules has a tendency to decrease rapidly. The problem is usually solved by the thermodesorption method combined with variation of the heating rate (by approximately not less than two orders of magnitude) or by the method of adsorption isobars (or isotherms). The most reliable data have apparently been obtained for the system CO/Ru (001).[109,110] Four methods were used to determine the parameters of the desorption rate constants. The results of different types of measurements agree satisfactorily with one another. It was established that the preexponential factor has a singularity for coverages at which the activation energy has a break (Fig. 13). In the case of the systems CO/Ir (110), NO/Pt (111), Ba/W (001) a compensating effect was found: as the coverage increases the activation energy and the preexponential factor both decrease (see, for example, Fig. 14); thus the preexponential factor partially compensates the increase in the rate of desorption, accompanying an increase in the coverage, owing to the decrease in the desorption activation energy. Data for the system CO/Ni (111) are inconsistent: according to Ref. 108 as the coverage increases the desorption activation energies decrease, and

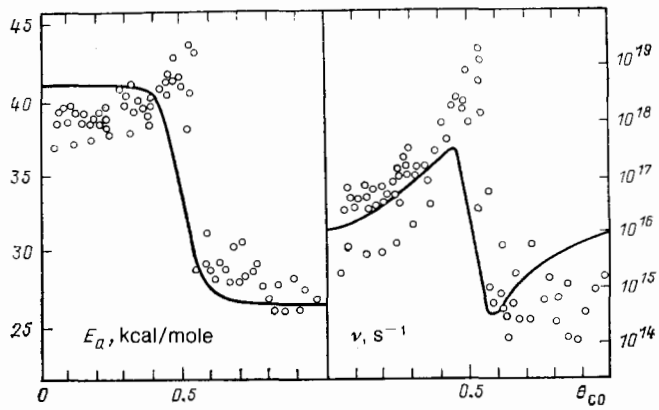

FIG. 13. The dependence of the activation energy and of the preexponential factor in the desorption rate constant on the coverage for the system CO/Ru (001). The circles show the experimental points,[109,110] and the solid lines correspond to the theory of Ref. 94.

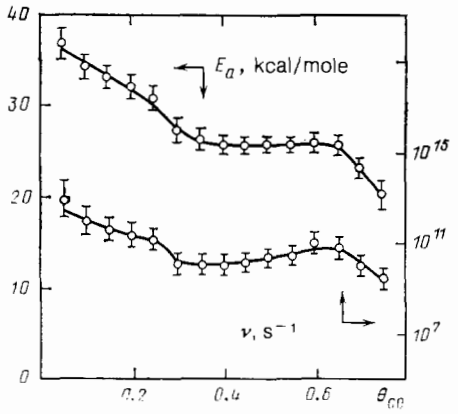

FIG. 14. The activation energy and the preexponential factor in the desorption rate constant as functions of the coverage for the system CO/Ir (110).[111,112]

the preexponential factor remains approximately constant; it was found in Ref. 113 that as the coverage increases the preexponential factor increases approximately by four orders of magnitude, while the activation energy remains constant.

Experimental investigations[108-113] stimulated theoretical work,[88,89,94] in which the effect of lateral interactions between adsorbed molecules on the preexponential factor in the desorption rate constant was analyzed with the help of the lattice-gas model. It turned out that lateral interactions have a substantial effect on the dependence of the preexponential factor on the coverage when $\varepsilon_1 \gg kT$. In particular, in the case of a square lattice, when repulsive lateral interactions between nearest neighbors are taken into account, the dependence of the desorption activation energy and of the preexponential factor on the coverage has the form[94,97]

$$E_a(\theta) = E_a(0), \quad \frac{\nu(\theta)}{\nu(0)} \approx \left(\frac{1-\theta}{1-2\theta}\right)^4 \quad \text{for} \quad \theta < \frac{1}{2},$$
$$E_a(\theta) = E_a(0) - 4\varepsilon_1, \quad \frac{\nu(\theta)}{\nu(0)} \approx \left(\frac{2\theta-1}{\theta}\right)^4 \quad \text{for} \quad \theta > \frac{1}{2}. \tag{6.4}$$

The formulas (6.4) were obtained in the quasichemical approximation under the assumption that $|\theta - (1/2)| \gg \exp(-\varepsilon_1/kT)$, so that they are inapplicable near $\theta = 1/2$. The physical meaning of the result (6.1) can be understood starting from general formulas of the type (4.2). Consider, for example, the case $\theta < 1/2$. In this case, molecules on a square lattice can become arranged so that no molecule has a neighbor in adjacent cells. In the region $\varepsilon_1 \gg kT$ the probability for a molecule to have neighbors is exponentially small, but in this case the rate of desorption is exponentially high owing to the lateral interactions. The two exponential terms compensate one another, and as a result lateral interactions affect not only the desorption activation energy but the preexponential factor also.

For lattices of a different type, a break in the activation energy and singularities in the preexponential factor occur for other coverages, for example, in the case of a hexagonal lattice for $\theta = 1/3$ and $\theta = 2/3$.

The nature of the effect of lateral interactions on the preexponential factor is in good qualitative agreement with the experimental results for the system CO/Ru (001) (see Fig. 13). We emphasize that in Fig. 13 θ is the coverage normalized to the absolute maximum value of the experimental coverage $\theta_m = 2/3$. For this reason, the point $\theta = 1/2$ corresponds to the absolute coverage $\theta = 1/3$. The preexponential factor was calculated in the quasichemical approximation based on the formulas (6.2) and (6.3) without making the assumption that $|\theta - (1/2)| \gg \exp(-\varepsilon_1/kT)$. The theoretical curves are somewhat smoother than the experimental curves, apparently, for two reasons. First, only the interaction between nearest-neighbors was taken into account in the calculations. Second, the quasichemical approximation does not take into account fully the effect of correlation on the arrangement of the particles. In the case of attraction between neighboring molecules the dependence of the desorption activation energy and of the preexponential factor on the coverage at low temperatures has the form

$$E_a(\theta) = \text{const}, \quad \frac{\nu(\theta)}{\nu(0)} = \frac{1-\theta}{\theta}, \quad T < T_c. \tag{6.5}$$

These formulas hold in the region of coexistence of the surface gas and the surface liquid. The physical significance of the formulas (6.5) is as follows. Desorption at temperatures $T < T_c$ occurs primarily from the surface-gas phase[5]; the volume of the surface gas is proportional to $(1-\theta)$, where θ is the total coverage of the surface; and, the rate of desorption is proportional to $R_d \sim \nu(\theta)\theta \sim (1-\theta)$. The rate of adsorption is also proportional to $1-\theta$. It follows from here, in particular, that in adsorption equilibrium and at a fixed temperature the surface gas and the surface liquid can coexist only at a strictly determined pressure in the volume phase.

We shall now discuss briefly the compensation effect. In the lattice-gas model the compensation effect apparently cannot be explained taking into account solely the lateral interactions (i.e., neglecting the dynamics). At the present time there do not exist lucid models explaining the compensation effect in the case of chemisorption. The compensation effect was predicted theoretically[116] for physically adsorbed particles, but, as the authors themselves emphasize, the arguments in Ref. 116 are useless in the case of chemisorption. In some articles[112] the compensation effect is explained formally on the basis of the theory of absolute reaction rates by the strong dependence on the coverage of the partition functions of the activated complex or of the adsorbed molecules. Such explanations do not clarify the situation as long as the reasons for the above-mentioned dependence are not indicated.

In discussing the compensation effect the accuracy of the experimental measurements should also be considered. An elementary analysis gives the following relationship between δE_a (the accuracy of the measurements of the activation energy of the process) and $\delta\theta$ (the accuracy of measurements of the coverage):

$$\delta E_a \approx \frac{T}{\Delta T} \frac{\partial E_a(\theta)}{\partial \theta} \delta\theta;$$

where T is the working temperature and ΔT is the tempera-

ture range in which the rate of the process is measured. Usually $T/\Delta T \gtrsim 4$, so that small systematic errors in the measurement of the coverage can cause substantial errors in the activation energy and the preexponential factor of the desorption rate constant. This could result in a false compensation effect. Unfortunately, the accuracy of coverage measurements is usually not discussed in experimental articles.

Summarizing, we note that systematic experimental and theoretical studies of the dependences on the coverage of the parameters in the rate constants of the simplest physical-chemical surface processes were begun only recently. Much remains unclear here. New experimental and theoretical work is required in order to gain a deeper understanding of how and on which factors the preexponential factors in the rate constants of surface processes depend. The magnitude of the preexponential factor, as is well known, is strongly affected by the dynamics of the motion of the nuclei. For this reason, in future theoretical studies of this problem the above-described (see Sec. 4) decoupling of the dynamic and statistical parts of the problem of calculating rate constants will have to be rejected.

7. THERMODESORPTION SPECTRA

The most widely used method for studying the kinetics of elementary surface processes is the thermodesorption method. The essence of thermodesorption measurements consists of the following. Molecules of one species (if desorption is studied) or molecules of two species (if a reaction is studied) are adsorbed on a surface at low temperatures, after which the chamber is evacuated and the sample is heated. Desorption or the reaction (followed by desorption of the reaction products) occurs as the temperature is raised, and the coverage of the surface decreases. The number of molecules entering the gas phase per unit time, i.e., actually the rate of the process of interest, is measured experimentally. The temperature dependence of the intensity of the measured signal is called the thermodesorption spectrum. The kinetics of the process can be studied for all values of the coverage—from complete coverage to zero coverage—in the course of a thermodesorption experiment over a short period of time. Analysis of thermodesorption spectra yields the dependence of the rate of the process of interest on the temperature and coverage. This is the advantage of the thermodesorption method and the reason for its widespread popularity.

The thermodesorption spectrum usually consists of one or several peaks. The most informative parameter, which makes it possible to evaluate the activation energy of the process, is the position of the thermodesorption peak. The formulas relating the position of the peak to the parameters in the rate constant of the process in the case of a process with "ideal" kinetics (i.e., the activation energy of the process does not depend on the coverage) were first derived in Ref. 117. The equations describing the "ideal" kinetics of some processes and the functional relationship between T_m (the temperature corresponding to the maximum of the rate of the process) and the parameters in the rate constant of the process are monomolecular desorption, as follows:

$$\frac{d\theta}{dt} = -\nu e^{-E_a/kT}\theta, \qquad e^{E_a/kT_m} = \nu\frac{kT_m^2}{\beta E_a}, \tag{7.1}$$

associative desorption,

$$\frac{d\theta}{dt} = -\nu e^{-E_a/kT}\theta^2, \qquad e^{E_a/kT_m} = \frac{2\theta_m \nu k T_m^2}{\beta E_a}, \tag{7.2}$$

and a bimolecular reaction between adsorbed molecules $A_s + B_s \rightarrow (AB)_{gas}$:

$$\frac{d\theta_A}{dt} = \frac{d\theta_B}{dt} = -\nu e^{-E_a/kT}\,\theta_A\theta_B, \qquad e^{E_a/kT_m} = \frac{(\theta_A+\theta_B)_m \nu k T_m^2}{\beta E_a}, \tag{7.3}$$

where β is the rate of heating, and the index m for the coverages indicates that the coverages are evaluated at the maximum of the rate of the process. Without loss of accuracy the formulas (7.1) and (7.2) can be somewhat simplified[117]:

$$\frac{E_a}{kT_m} = \ln\frac{\nu T_m}{\beta} - 3.64, \tag{7.1'}$$

$$\frac{E_a}{kT_m} = \ln\frac{\theta_0 \nu k T_m^2}{\beta E_a}, \tag{7.2'}$$

where θ_0 is the initial coverage.

In determining the activation energy using the formulas (7.1)–(7.3) the value of the preexponential factor must be postulated. The so-called "normal" values of the preexponential factors, $\nu \sim 10^{13}$–$10^{16}\,s^{-1}$, obtained using the theory of absolute reaction rates, are usually used in the calculations. The activation energy for real processes, as a rule, depends on the coverage. In this case, the relations (7.1)–(7.3) give the average value of the activation energy.

Another important parameter of the thermodesorption spectrum is the half-width of the peak. The analytical formulas relating the half-width of the thermodesorption peak to the parameters of the rate constant were obtained for the case of "ideal" kinetics in Ref. 118 by approximating the results of numerical calculations. These formulas are not, however, widely used, since the width of real thermodesorption peaks is affected substantially by the dependence of the desorption activation energy on the coverage, even if this dependence is weak. The computational results of Ref. 118, enabling the analysis of thermodesorption spectra under the assumption that the desorption activation energy depends linearly on the coverage, turned out to be more useful.

The possibility of reconstructing the dependence of the activation energy and the preexponential factor on the coverage from the form of the thermodesorption spectrum was discussed in Refs. 119–121. It was shown in Ref. 120 that when the real uncertainty in the thermodesorption spectra is taken into account, this problem cannot, as a rule, be solved uniquely. The problem can be solved[111] if the experiment is performed by varying (by two or more orders of magnitude) the rate of heating.

The effect of lateral interactions between adsorbed mol-

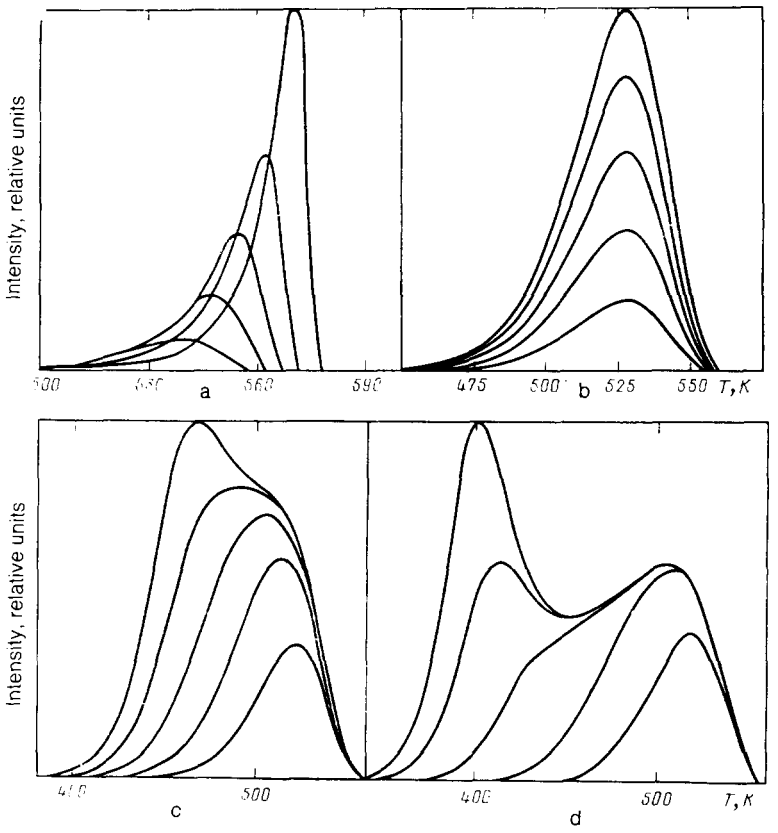

FIG. 15. Thermodesorption spectra in the case of monomolecular desorption. a) $\varepsilon_1 = -1$ kcal/mole; b) $\varepsilon_1 = 0$ kcal/mole; c) $\varepsilon_1 = 1$ kcal/mole; d) $\varepsilon_1 = 2$ kcal/mole. The initial coverages equal 0.2, 0.4, 0.6, 0.8, and 1.

ecules on the thermodesorption spectra was first discussed in Refs. 83 and 86. It was shown that lateral interactions can give rise not only to broadening of the thermodesorption peak, but also to the appearance of several peaks. The appearance of several peaks is due to the nonlinear dependence of the activation energy of the process on the coverage (see, for example, Fig. 13). References 83 and 86 substantially influenced the interpretation of thermodesorption spectra. The idea that the complicated form of thermodesorption spectra can be equally a consequence of both surface nonuniformity and lateral interactions between adsorbed molecules is now generally accepted.

The typical scale of the effect of lateral interactions on thermodesorption spectra of different processes is demonstrated below in Figs. 15–17. All calculations were carried out for a square lattice, taking into account the lateral interactions between nearest neighbors only. Aside from this, it is assumed that the activated complex does not interact with the environment ($\varepsilon_i^* = 0$). In the case of adsorption or reactions involving the formation of products which escape directly into the gas phase, this assumption is reasonable, since the activated complex in these processes is usually weakly bound to the surface. The starting temperature was set equal to 300 K, and the rate of heating equaled 50 K/s. The equations derived in Ref. 93 in the quasichemical approximation were used to describe the kinetics of the processes.

The thermodesorption spectra for monomolecular desorption, calculated with the parameters $E_a(0) = 35$ kcal/mole and $\nu = 10^{15}\ s^{-1}$, which are typical for the desorption of CO from the surface of platinum-group metals, are presented in Fig. 15. In the "ideal" case (see Fig. 15b) the position of the peaks is independent of the initial coverage. The attraction between molecules (see Fig. 15a) gives rise to behavior which is characteristic for zeroth-order desorption: the rate of the process is virtually independent of the initial coverage. Moderate repulsion ($\varepsilon_1 = 1$ kcal/mole) between adsorbed molecules causes a weak splitting of the spectrum (see Fig. 15c). Comparatively strong repulsion ($\varepsilon_1 = 2$ kcal/mole) leads to the appearance of two distinct peaks (see Fig. 15d); the integral intensities of the peaks are equal to one another—this is another consequence of the symmetry of the lattice gas model with pair interactions relative to the coverage $\theta = 1/2$ mentioned in Sec. 2. Taking into account the second interaction ε_2 does not qualitatively change the thermodesorption spectra.[95] When three-body interactions[122] are taken into account the integral intensities of the peaks are no longer equal. In the case of other types of lattices the quasichemical approximation gives the correct results only for weak lateral interactions. Detailed calculations of thermodesorption spectra for more complicated lattices than the square lattice have not been performed.

The thermodesorption spectra for associative desorption, calculated with the parameters $E_a(0) = 65$ kcal/mole and $\nu = 10^{13}\ s^{-1}$, typical for desorption of oxygen atoms from the surface of platinum-group metals, are presented in Fig. 16. Here, lateral interactions of the same magnitude as in the case of monomolecular desorption studied above have a somewhat weaker effect on the thermodesorption spec-

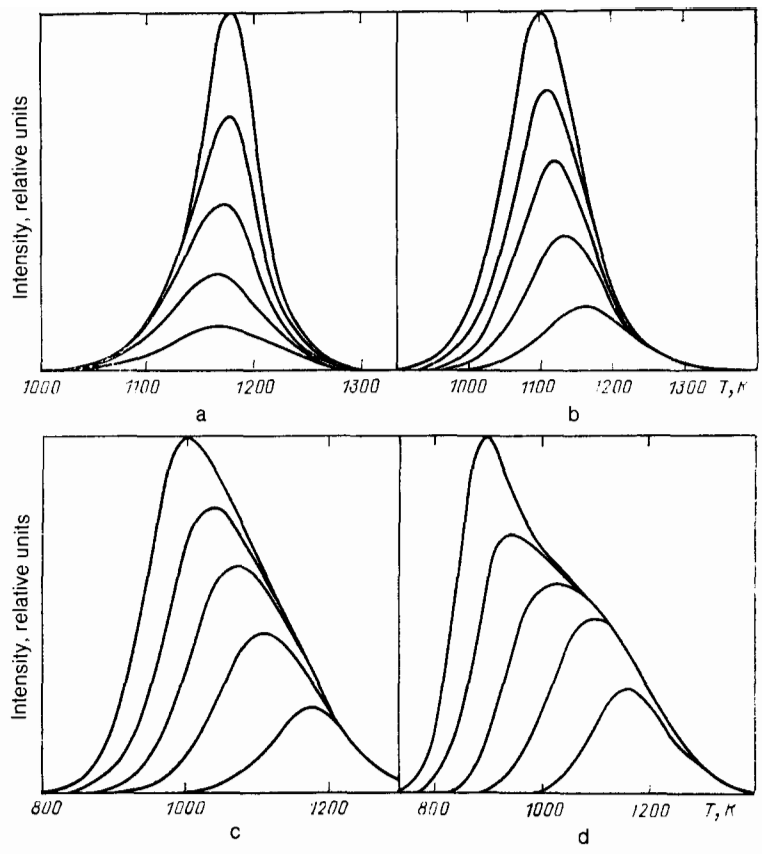

FIG. 16. Thermodesorption spectra in the case of associative desorption. a) $\varepsilon_1 = -1$ kcal/mole; b) $\varepsilon_1 = 0$ kcal/mole; c) $\varepsilon_1 = 1$ kcal/mole; d) $\varepsilon_1 = 2$ kcal/mole. The initial coverages equal 0.2, 0.4, 0.6, 0.8, and 1.

trum. This is attributable to the fact that, owing to the high activation energy, oxygen is desorbed at high temperatures and the dimensionless parameter ε_1/kT, which affects the nature of the thermodesorption spectrum, is small. The thermodesorption spectra for associative desorption of particles of one species in the presence of particles of a different species on the surface are analyzed in detail in Ref. 95, in which the thermodesorption spectra under the conditions of decomposition of NO on platinum-group metals are analyzed (see the discussion of this point in Sec. 4 also).

The thermodesorption spectra for the bimolecular reaction $A_s + B_s \rightarrow (AB)_{gas}$, between the adsorbed molecules, calculated in Ref. 123 with the parameters $E_a(0) = 35$ kcal/mole and $\nu = 10^{14}$ s, are presented in Fig. 17. The energies of different lateral interactions were assumed to be equal to one another: $\varepsilon_{AA} = \varepsilon_{AB} = \varepsilon_{BB}$. Two families of thermodesorption spectra were analyzed. In the first case, the initial coverage of the surface by the B molecules equals $\theta_B = 0.2$, and the initial coverage of the surface by the A molecules assumes the values 0.8, 0.6, 0.4, 0.2, and 0.1. In the second case $\theta_B = 0.5$, while θ_A assumes the values 0.5, 0.4, 0.3, 0.2, and 0.1. The spectra in the first and second families were normalized independently. A detailed discussion of the qualitative features of the spectra, presented in Fig. 17, is given in Ref. 123.

Figures 15–17 give a general idea of the effect of lateral interactions on thermodesorption spectra. In many articles (Table II) the lattice-gas model was used to describe real thermodesorption spectra. Experience accumulated thus far indicates that the experimental results can usually be described at the semiquantitative level only. This is apparently attributable to the fact that in almost all theoretical papers the lateral interactions between nearest neighbors only were taken into account; in addition, the arrangement of the molecules on the surface was often assumed to be simpler than that occurring in reality. In future, attempts will apparently be made to describe the experimental results taking into account lateral interactions of a more complicated type. There are no fundamental difficulties here; only more computer time is required.

Real thermodesorption spectra are often nonideal as a result of surface nonuniformity also, i.e., the presence on the surface of several forms of adsorbed molecules or even a continuous description of adsorbed molecules as a function of their surface binding energy. Generally speaking, surface nonuniformity is apparently a more common reason for the nonideality of thermodesorption spectra, especially in the case of desorption from polycrystalline surfaces. Both surface nonuniformity and lateral interactions produce effects of the same order of magnitude in the thermodesorption spectra. In many cases both surface nonuniformity and lateral interactions are apparently manifested simultaneously. If, however, one of the factors responsible for the nonideality of thermodesorption spectra dominates, then this factor can in principle be established experimentally. The classical example here is the isotopic method, consisting of the successive adsorption of different isotopes, followed by their desorption. If different isotopic molecules are desorbed in an

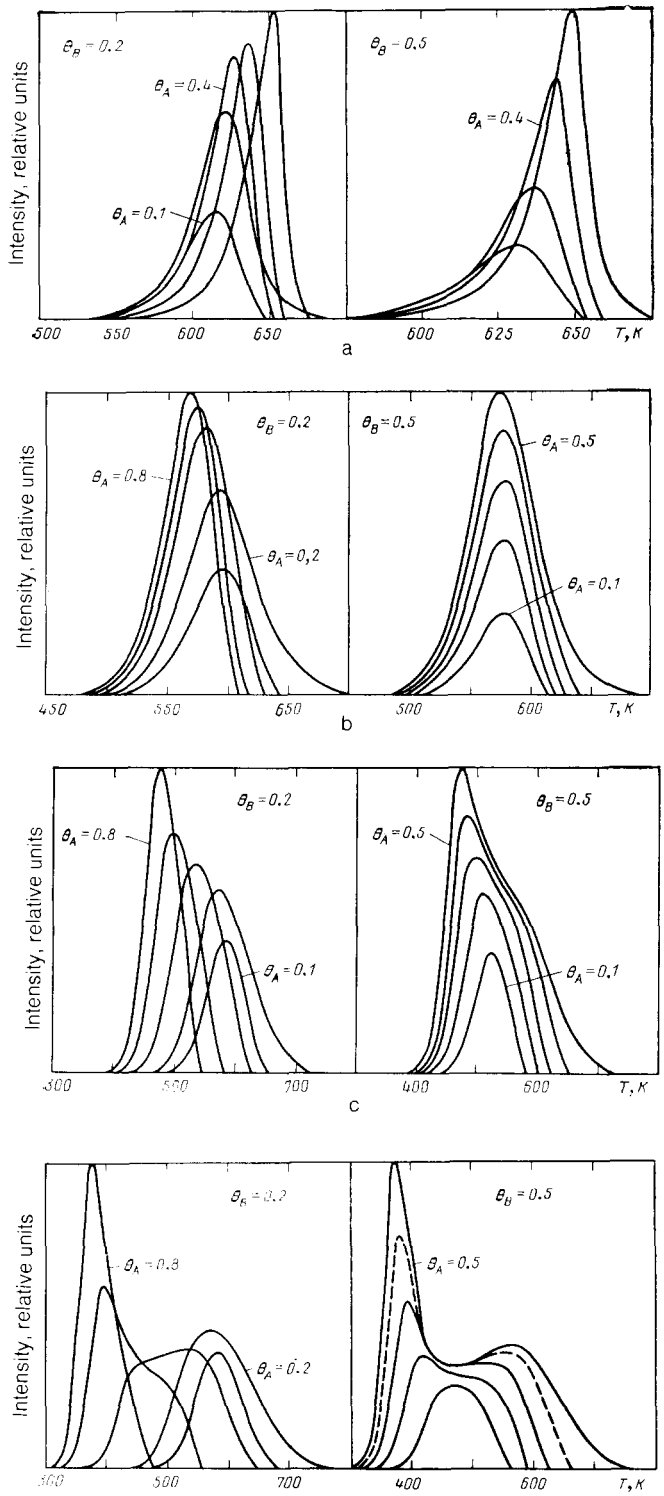

FIG. 17. a–d) Thermodesorption spectra in the case of a bimolecular reaction between adsorbed molecules. a) $\varepsilon_1 = -1$ kcal/mole; b) $\varepsilon_1 = 0$ kcal/mole; c) $\varepsilon_1 = 1$ kcal/mole; d) $\varepsilon_1 = 2$ kcal/mole.

order inverse to that in which they were adsorbed, then the surface is obviously nonuniform. Unfortunately, the isotopic method gives no information in the case when the transitions of molecules from one form into another occur more rapidly than does desorption from different forms. In the latest methods for studying surface nonuniformity different forms of the adsorbed molecules are recorded directly (with the help, for example, of infrared spectra, photoelectronic spectra, or spectra of the energy losses in low-energy electron scattering).

8. ISOTHERMAL KINETICS

Together with thermodesorption measurements, the nonstationary kinetics of elementary surface processes is often studied under isothermal conditions (see references given in Refs. 136 and 137). The experimental nonstationary isothermal kinetic data usually cannot be described on the basis of "ideal" kinetics. This is partially attributable to the lateral interactions between the adsorbed particles. The effect of lateral interactions on isothermal kinetics has been discussed qualitatively in many experimental works. Detailed calculations of the isothermal kinetics of monomolecular desorption, associative desorption, and the bimolecular reaction $A_s + B_s \rightarrow (AB)_{gas}$ were carried out in Refs. 136 and 137. It was shown that taking into account lateral interactions gives kinetic curves of two types (see, for example, Fig. 18). In the first case, the coverage of the surface decreases rapidly initially, after which the desorption process or the reaction slows down markedly. In the second case, an induction period is observed initially, after which the process is accelerated. For monomolecular and associative desorption the kinetic curves of the first type occur for repulsive interactions between adsorbed molecules, and kinetic curves of the second type occur for attractive interactions. For the bimolecular reaction proceeding according to the Langmuir-Hinshelwood mechanism, kinetic curves of both types are possible with both positive and negative lateral interactions. Physically, the features mentioned above are a result of the coverage-dependence of the activation energy of the processes.

The features of isothermal kinetics described above are traditionally explained by invoking either complicated kinetic schemes, including, for example, topochemical stages (growth and destruction of patches), or surface nonuniformity. The calculations carried out in Refs. 136 and 137 show that the complicated nature of the isothermal kinetics can also be a consequence of lateral interactions between adsorbed molecules.

9. SURFACE DIFFUSION

Surface diffusion is of interest from the general physical standpoint as an example of diffusion in strongly nonideal systems. In addition, information about surface diffusion is useful for describing chemical reactions on a surface. Surface diffusion is characterized, as a rule, by times which are significantly shorter than desorption times, since the activation energy of diffusion hopping is usually less than or of the order of 30% of the desorption activation energy. Nevertheless, surface diffusion can have a nontrivial effect on the kinetics of surface chemical reactions.

Indeed, molecules or atoms of different species usually participate in reactions, and diffusion of the particles which are most strongly bound to the surface can, in principle, be

TABLE II. List of references in which the lattice-gas model was used for interpreting the thermodesorption spectra.

Monomolecular desorption		Associative desorption	
System	References	System	References
Hg/W (001)	125	O_2/Ag (110)	129
CO/W (210)	86	H_2/W (001)	86, 162
CO/Ir (110)	126, 135	N_2/W (001)	86
CO/Ir (111)	127, 135	O_2/Ir (110)	126, 135
CO/Pt (111)	135	O_2/Ir (111)	127, 135
CO/Pt (110)	135	H_2/Pt (111)	128
CO/Pd (111)	135	O_2/Pt (001)	130
		O_2/Pt (111)	135
		O_2/Pd (111)	135
		H_2/Ni (100)	131

Chemical reactions		
Process	Surface	References
Oxidation of CO	Ir (110), Ir (111)	126, 127
Oxidation of H_2	Pt (111)	128
Decomposition of NO	Co, Ni, Ru, Re	90, 91, 95, 132
Decomposition of HCOOH	Ni (110), Ni (100)	133, 134
Oxidation of methanol	Ag (110)	133

slower than desorption of less weakly bound particles or a reaction. For example, the diffusion of oxygen atoms on a transition-metal surface at temperatures $T < 400$ K is characterized by times exceeding tens of seconds. Such times can be long compared with desorption times for weakly bound reagents or with reaction times. For this reason, the arrangement of oxygen atoms on the surface at temperatures $T < 400$ K is often unbalanced. In this case, the correct description of the adsorption layer in the course of the oxidative reaction must include a detailed microscopic analysis of the displacements of different particles along the surface (i.e., the calculation of the probabilities of different configurations of the arrangements of adsorbed particles).[100]

Aside from the unbalanced nature of the adsorbed layer described above relative to the arrangement of strongly bound particles, information about surface diffusion is required for describing diffusion-controlled chemical reactions. For example, a reaction can occur only on separate sections of the surface (the so-called active centers). Diffusion of reagents toward active centers can in principle limit the reaction. Formal models of such processes are studied in Refs. 138–140. Unfortunately, as far as we know, at the present time there are no reliable data indicating real reactions to which the models of Refs. 138–140 are applicable.

Considerable attention has been devoted in recent years to the experimental and theoretical study of the diffusion of adsorbed atoms and of the simplest molecules.[84,137,141–159] Two experimental methods for studying the dependence of the coefficient of surface diffusion[6)] on the coverage are widely used. The first method for determining the coefficient of diffusion is based[142] on the measurement of fluctuations in the number of particles on a selected section of the surface followed by the use of relations (of the Smoluchowski type) between the coefficient of diffusion and the rate of fluctuation of the concentration. The second method[143] reduces to measuring the concentration profile of the particles diffusing from the occupied half-plane into the free half-plane and then using the Boltzmann-Matano procedure for determining the diffusion coefficient. Neither method is rigorously substantiated. The first method is limited by the fact that there are no sufficiently accurate and simple relations between the rate of fluctuation of the concentration and the

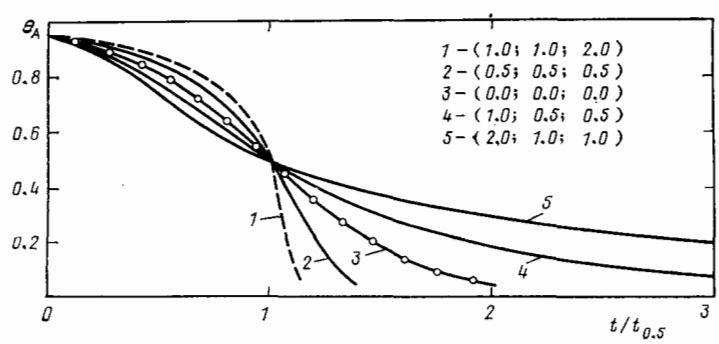

FIG. 18. Time dependence of the coverage of the surface by A molecules in the case of the reaction $A_s + B_s \rightarrow (AS)_{gas}$. It is assumed that the concentration of B molecules in the gas phase is high, so that the B molecules occupy all locations on the surface freed in the course of the reaction, i.e., the condition $\theta_A + \theta_B = 1$ holds at all times. The calculation was performed for a square lattice. The notation (2, 0; 1, 0; 1, 0) denotes $\varepsilon_{AA}/kT = 2.0$; $\varepsilon_{AB}/kT = 1.0$; $\varepsilon_{BB}/kT = 1.0$.

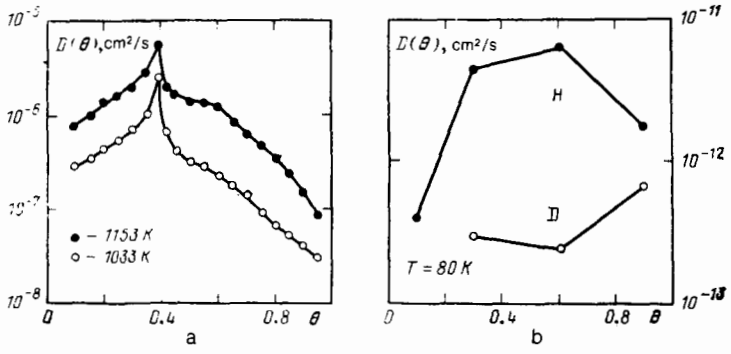

FIG. 19. Dependence of the diffusion coefficient on the coverage for the systems O/W (110)[143] (a) and H/W (110), D/W (110)[144] (b).

diffusion coefficient in the case of interacting molecules. The second method is based on the assumption that the concentration profile $c(x,t)$ is a function of the parameter $x/t^{1/2}$ only. This assumption must be checked experimentally, since it is justified theoretically only in the case of noninteracting particles.

The experimetnally measured diffusion coefficients depend very strongly on the coverage of the surface by the diffusing particles (see, for example, Fig. 19). One reason for this are the lateral interactions between the adsorbed particles. The effect of lateral interactions on the diffusion was discussed in Refs. 84, 137, and 146–159, where different approximations or the Monte Carlo method were used. Some papers (for example, Refs. 84, 146, and 148) were based on obviously simplified models of the effect of intermolecular interactions on diffusion. The exact expression relating the flux of adsorbed particles to the concentration gradient has the form

$$J = -D(\theta)\frac{\partial c}{\partial} = -a^2\Gamma(\theta)\frac{z}{4}\frac{\theta}{kT}\frac{\partial\mu}{\partial\theta}\frac{\partial c}{\partial x}, \qquad (9.1)$$

where a is the distance between neighboring cells, z is the number of neighboring cells, $\Gamma(\theta)$ is the probability per unit time of hopping into one of the neighboring cells, and $\mu(\theta)$ is the chemical potential. The formula (9.1) was derived phenomenologically.[149,150] A simple kinetic derivation of the formula (9.1) is given in Refs. 137 and 157. The expression (9.1) for the coefficient of diffusion is valid if the diffusion occurs as a result of individual hops. This is the case if for a diffusion hop the particle must overcome an activation barrier (in this case, the probability that adjacent particles make a hop simultaneously is negligibly small). It is this situation that, as a rule, occurs in the case of chemisorption.

The results of the calculations carried out in Ref. 137, illustrating the effect of different types of lateral interactions on the dependence of the diffusion coefficient on the coverage, are presented in Figs. 20 and 21. In accordance with experiment, the theory gives a strong dependence of the diffusion coefficients on the coverage, and it also predicts the possibility that this dependence is nonmonotonic. The nonmonotonic nature of the dependence of the diffusion coefficient on the coverage is linked with the fact that the different factors entering into the formula (9.1) depend differently on the coverage.

There is practically no experience at the present time in the use of the lattice-gas model for describing real data on surface diffusion rates. This is attributable to two factors. On the one hand, there are as yet few experimental data on the coverage dependences of diffusion coefficients. On the other hand, in order to describe existing data lateral interactions of a complicated type must be taken into account. In the case, for example, of the diffusion of oxygen in the W (110) face this fact already follows from the form of the phase diagram of the system (see Fig. 4). Model calculations of the diffusion of oxygen on the W (110) surface were carried out in Ref. 156.

The formula (9.1) describes diffusion occurring as a result of individual hops of separate molecules into adjacent free cells. The possibility of molelcules hopping in pairs was discussed in Ref. 158. In Ref. 154, together with this possi-

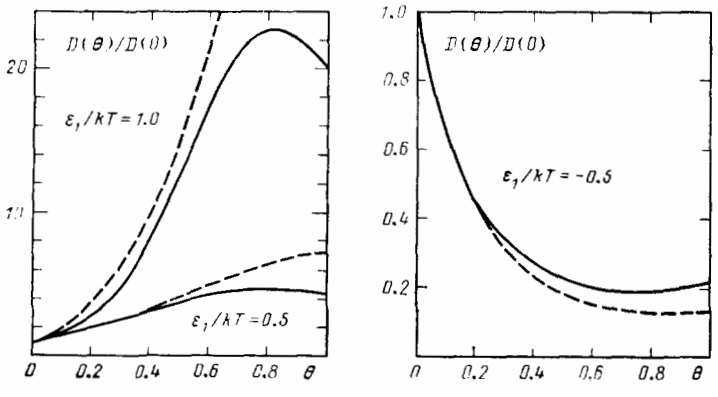

FIG. 20. The diffusion coefficient as a function of the coverage, taking into account lateral interactions between nearest neighbors. The calculation was performed for a square lattice. The broken lines correspond to the mean-field approximation and the solid lines correspond to the quasichemical approximation.

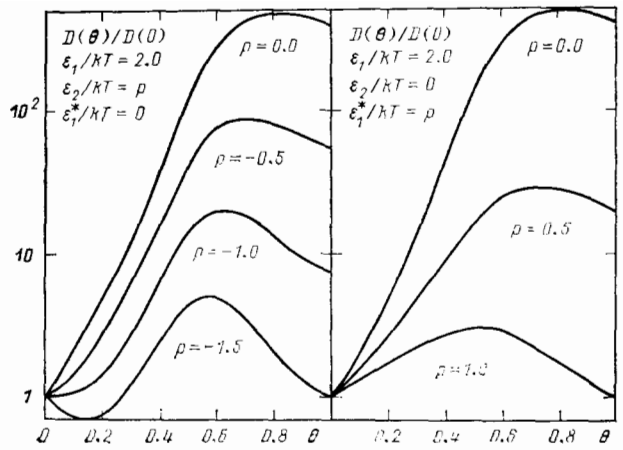

FIG. 21. The diffusion coefficient as a function of the coverage taking into account lateral interactions, ε_1 and ε_2 are the lateral interactions between adsorbed molecules; ε_1^* is the lateral interaction of the activated complex with nearest neighbors. The calculation was carried out for a square lattice.

bility, the so-called "chain" mechanism of diffusion was studied. The idea of chain diffusion dates back to Ref. 160. The essence of this mechanism reduces to the fact that hops into occupied cells are permitted, and in addition it is assumed that as a result of such a hop molecules already present in an occupied cell are "pushed out" into a neighboring cell, etc. In our opinion the chain mechanism of diffusion has not been adequately substantiated. This mechanism could be important, if the activation energy of the process of displacement of molecules is lower than the activation energy of hopping into a neighboring empty cell. It is difficult, however, to imagine that such a ratio between the activation energies can be realized in reality.

The effect of the order-disorder phase transition on surface diffusion was studied in Ref. 153. It was shown that in the case when a (2×1) structure is formed on a square lattice the diffusion coefficient becomes strongly anisotropic. From the physical standpoint this result is completely natural.

10. CONCLUSIONS

The information collected in this review indicates that over the last decade the two-dimensional lattice-gas model came into widespread use for describing different phenomena occurring on the surfaces of single crystals. Interest in this model will persist in the immediate future. Indeed, surface physics is going through a blossoming period; an enormous amount of experimental data here requires theoretical interpretation. From the methodological standpoint further development of the two-dimensional lattice-gas model will apparently be linked with more extensive use of the Monte Carlo method not only for calculating the phase diagrams of the adsorbed layer, but also for describing the kinetics of different surface processes.

In concluding this review it should apparently be emphasized that our exposition was based primarily on the analysis of the applications of the lattice-gas model for describing surface phenomena. In this model the surface is assumed to be uniform. For this reason, we did not discuss surface nonuniformity in detail. However, the effect of surface nonuniformity on surface phenomena is often significant even in the case of adsorption on surfaces of single crystals. There is a large volume of experimental data on adsorption on nonuniform surfaces. Interest in the theory of the phenomena occurring on nonuniform surfaces is also increasing. Analysis of such questions, however, falls outside the scope of this review.

In conclusion, we are deeply grateful to V. L. Pokrovskiĭ for useful discussions of the material collected in this review and for a number of valuable remarks.

[1)]Review lecture presented at the 1st All-Union Symposium on Theoretical Problems in Chemical Physics, Chernogolovka, Moscow Province, June 11–14, 1984.

[2)]Physical adsorption is discussed in the reviews of Refs. 6 and 7.

[3)]One of the consequences of lateral interactions between an activated complex and the environment can be the dependence on the coverage of the average energy (translational, vibrational, or rotational) of the products of desorption from the surface. This effect is studied in Ref. 163.

[4)]We note that the formula (47) in Ref. 93 contains a misprint. The correct expression for the braces has the form $\{...\} = K_{ca} + K_{cd} + K_{cf}P_{ef}K_{fd}/(K_{fe}P_{fe} + K_{fd})$.

[5)]In the case, for example, of a square lattice the ratio of the density of the surface gas to that of the surface liquid equals $\approx\exp(2\varepsilon_1/kT)$ (see Sec. 2), while the ratio of the rate constant for desorption from the surface gas to that for desorption from liquid equals $\approx\exp(4\varepsilon_1/kT)$. It is clear from here that desorption occurs primarily from the surface gas.

[6)]We do not study here the diffusion of separate atoms, since the description of diffusion in the limit of low coverage is a purely dynamic problem.

[1]L. D. Roelofs, Chemistry and Physics of Solid Surface, IV, Springer-Verlag, New York (1982), p. 219 (Springer Series on Chemical Physics, Vol. 20).
[2]T. L. Einstein, *ibid.*, p. 251.
[3]L. D. Roelofs and P. J. Estrup. Surf. Sci. **125**, 51 (1983).
[4]W. H. Weinberg, Ann. Rev. Phys. Chem. **34**, 217 (1983).
[5]D. P. Woodruff, G. C. Wang, and T. M. Lu, The Chemical Physics of Solid Surfaces and Heterogeneous Catalysis, Elsevier, Amsterdam (1983), Vol. 2, p. 252.
[6]A. Thomy, X. Duval, and J. Regnier, Surf. Sci. Rept. **1**, 1 (1981).
[7]M. Bienfait, Dynamics of Gas-Solid Interactions, Springer-Verlag, New York (1982), p. 94.
[8]Spektroskopiya i difraktsiya élektronov pri issledovanii poverkhnosti tverdykh tel (Spectroscopy and Diffraction of Electrons in the Study of the Surfaces of Solids), Nauka, Moscow (1985).
[9]D. G. Castner and G. A. Somorjai, Chem. Rev. **79**, 233 (1979).
[10]L. D. Landau and E. M. Lifshitz, Statisticheskaya fizika, Nauka, M., 1976 [Engl. transl., Statistical Physis, Pergamon Press, Oxford, 1980].
[11]V. L. Pokrovskiĭ and A. L. Talapov, Zh. Eksp. Teor. Fiz. **78**, 269 (1980) [Sov. Phys. JETP **51**, 134 (1980)].
[12]V. L. Pokrovsky and A. L. Talapov, Phys. Rev. Lett. **42**, 65 (1979).
[13]S. N. Coppersmith, D. S. Fisher, B. I. Halperin, P. A. Lee, and W. F. Brinkman, *ibid.* **46**, 549 (1981); Phys. Rev. B **25**, 349 (1982).
[14]J. Villa and P. Bak, J. Phys. (Paris) **42**, 657 (1981).
[15]S. T. Chui, Phys. Rev. B **23**, 5928 (1981).
[16]M. Kardar and A. N. Berker, Phys. Rev. Lett. **48**, 1552 (1982).
[17]E. Domany, M. Schick, and J. S. Walker, Phys. Rev. B **18**, 2209 (1978); **20**, 3828 (1979).
[18]C. Rootman, *ibid.* **24**, 1482 (1981).
[19]M. Schick, Progr. Surf. Sci. **11**, 245 (1981).
[20]T. Einstein J. Gertz, and J. Schrieffer, in: Theory of Chemisorption, J. R. Smith, Springer-Verlag, Berlin, 1980 [Russ. transl., Mir, M., 1983, p. 256].
[21]M. I. Urbakh and A. M. Brodskiĭ, Zh. Fiz. Khim. **59**, 1152 (1985).
[22]J. P. Muscat and D. M. Newns, Surf. Sci. **105**, 570 (1981); **110**, 85.
[23]E. Ruckenstein and T. Halvachev, *ibid.* **122**, 422 (1982).
[24]R. Baxter, Exactly Solved Models in Statistical Mechanics, Academic Press, N. Y., 1982 [Russ. transl., Mir, M., 1985].
[25]A. Z. Patashinskiĭ and V. L. Pokrovskiĭ, Fluktuatsionnaya teoriya fazo-

vykh perekhodov, Nauka, M., 1982 [Engl. transl. of earlier edition, Fluctuation Theory of Phase Transitions, Pergamon Press, Oxford, 1979].
[26]K. Binder and D.P. Landau, Surf. Sci. **61**, 577 (1976).
[27]F. Claro and V. Kumar, *ibid.* **119**, L371 (1982).
[28]K. Binder, W. Kinzel, and D. P. Landau, *ibid.* **117**, 232.
[29]P. J. Behm, K. Christmann, and G. Ertl, *ibid.* **99**, 320 (1980).
[30]K. Binder and D. P. Landau, *ibid.* **108**, 503 (1981).
[31]T. M. Lu, G. C. Wang, and M. G. Lagally, *ibid.* **92**, 133 (1980).
[32]E. D. Williams, S. L. Cunningham, and W. H. Weinberg, J. Chem. Phys. **68**, 4688 (1978).
[33]R. Imbiche, R. J. Behm, K. Christmann, and G. Ertl. Surf. Sci. **117**, 257 (1982).
[34]W. Kinzel, W. Selke, and K. Binder, *ibid.* **121**, 13.
[35]W. Selke, K. Binder, and W. Kinzel, *ibid.* **125**, 74 (1983).
[36]D. P. Landau, Phys. Rev. B **27**, 5604 (1983).
[37]L. D. Roelofs, A. R. Kortan, T.L. Einstein, and R. L. Park, J. Vac. Sci. Technol. **18**, 492 (1981).
[38]E. Domany, M. Schick, and J. S. Walker, Solid State Commun. **30**, 331 (1979).
[39]K. Nagai, Surf. Sci. **136**, 614 (1984).
[40]K. Nagai, Y. Ohno, and T. Nakamura, Phys. Rev. B **30**, 331 (1979).
[41]L. D. Roelofs, A. R. Kortan, and T. L. Einstein, Phys. Rev. Lett. **46**, 1465 (1981).
[42]I. F. Lyuksyutov and A. G. Fedorus, Zh. Eksp. Teor. Fiz. **80**, 2511 (1981) [Sov. Phys. JETP **53**, 1317 (1981)].
[43]A. G. Fedorus and V. V. Gonchar, Surf. Sci. **140**, 499 (1984).
[44]G. C. Wang and T. M. Lu, Phys. Rev. B **31**, 5918 (1985).
[45]K. Christmann, R. J. Behm, and G. Ertl, J. Chem. Phys. **70**, 4168 (1979).
[46]A. R. Kortan and R. L. Park, Phys. Rev. B **23**, 6340 (1981).
[47]D. E. Taylor and R. L. Park, Surf. Sci. **125**, L73 (1983).
[48]P. J. Estrup. J. Vac. Sci. Technol. **16**, 635 (1979).
[49]E. D. Williams, W. H. Weinberg, and A. C. Subrero, J. Chem. Phys. **76**, 1150 (1982).
[50]G. Ertl and P. Rau, Surf. Sci. **15**, 443 (1969).
[51]G. Ertl and J. Kuppers, *ibid.* **21**, 61 (1970).
[52]P. Rujan, W. Selke, and G. Uimin, Z. Phys. K1, B **53**, 221 (1983).
[53]R. A. Barker and P. J. Estrup, J. Chem. Phys. **74**, 1442 (1982).
[54]K. H. Lau and S. C. Ying, Phys. Rev. Lett. **44**, 1222 (1980).
[55]S. C. Ying and L. D. Roelofs, Surf. Sci. **125**, 218 (1983).
[56]L. D. Roelofs and S. C. Ying, *ibid.* **147**, 203 (1984).
[57]T. Inaoka and A. Yoshimori, *ibid.* **115**, 301 (1982).
[58]G. C. Wang and T. M. Lu, Phys. Rev. B **28**, 6795 (1983).
[59]V. K. Medvedev, A. G. Naumovets, and A. G. Fedorus, Fiz. Tverd. Tela (Leningrad) **12**, 375 (1970) [Sov. Phys. Solid State **12**, 301 (1970)].
[60]J. Kuppers and H. Michel, Appl. Surf. Sci. **3**, 179 (1979).
[61]M. Grunze, P. H. Kleban, W. M. Unertl, and F. S. Rys, Phys. Rev. Lett. **51**, 582 (1983).
[62]J. Kolaczkiewicz and E. Bauer, *ibid.* **53**, 485 (1984).
[63]T. E. Jackman, P. R. Norton, D. P. Jackson, and J. A. Davies, J. Vac. Sci. Technol. **20**, 607 (1982).
[64]D. L. Doering and S. Semancik, Surf. Sci. **129**, 177 (1983).
[65]R. J. Behm, P. A. Thiel, P. R. Norton, and G. Ertl, J. Chem. Phys. **78**, 7437 (1983).
[66]P. R. Norton, J . A. Davies, D. K. Creber, C. W. Sitter, and T. E. Jackman, Surf. Sci. **108**, 205 (1981).
[67]V. P. Zhdanov, *ibid.* **164**, L807 (1985).
[68]V. P. Zhdanov, Kinet. Kataliz. **27**, 597 (1986).
[69]V. A. Sobyanin, G. K. Boreskov, and A. R. Cholach, Dokl. Akad. Nauk SSSR **279**, 1410 (1984).
[70]M. P. Cox, G. Ertl, R. Imbichl, and J. Rustig, Surf. Sci. **134**, L517 (1983).
[71]P. R. Norton, P. E. Binder, K. Griffiths, T. E. Jackman *et al.*, J. Chem. Phys. **80**, 3859 (1984).
[72]P. A. Rikvold, Phys. Rev. B **32**, 4756 (1985).
[73]A. Sadiq and K. Binder, J. Stat. Phys. **35**, 517 (1984).
[74]E. T. Gawlinski, M. Grant, J. D. Gunton, and K. Kaski, Phys. Rev. B **31**, 281 (1985).
[75]I. M. Lifshitz, Zh. Eksp. Teor. Fiz. **42**, 1354 (1962) [Sov. Phys. JETP **15**, 1939 (1962)].
[76]J. E. Inglesfield, Vacuum **31**, 663 (1981).
[77]I. Terakura, K. Terakura, and N. Hamada, Surf. Sci. **103**, 103 (1981).
[78]J. C. Tully, Ann. Rev. Phys. Chem. **31**, 319 (1980).
[79]V. P. Zhdanov and K. I. Zamaraev, Catal. Rev. **24**, 373 (1982); Z. Knor, Physics of Solid Surfaces, Elsevier, Amsterdam (1985), p. 71; M. J. Cardillo, Langmuir **1**, 4 (1985).
[80]V. P. Zhdanov and K. I. Zamaraev, Zh. Fiz. Khim. **59**, 1112 (1985).
[81]J. K. Roberts, Proc. R. Soc. London A **161**, 141 (1937).
[82]T. Toya, J. Vac. Sci. Technol. **9**, 11 (1972).
[83]C. G. Goymour and D. A. King, J. Chem. Soc. Farad. Trans. Ser. 1 **69**, 749 (1973).
[84]D. A. King, Crit. Rev. Sol. State Mater. Sci. Trans. **7**, 167 (1978).
[85]A. Cassuto and D. A. King, Surf. Sci. **102**, 388 (1981).
[86]D. L. Adams, *ibid.* **42**, 12 (1974).
[87]D. A. King and M. G. Wells, Proc. R. Soc. London A **339**, 245 (1974).
[88]P. K. Johansson, Chem. Phys. Lett. **65**, 366 (1979).
[89]U. Leuthausser, Z. Phys. K1. B **37**, 65 (1980).
[90]M. E. Bridge and R. M. Lambert, Proc. R. Soc. London A **370**, 545 (1980).
[91]M. E. Bridge and R. M. Lambert, Surf. Sci. **94**, 469 (1980).
[92]V.P. Zhdanov, *ibid.* **102**, L35 (1981).
[93]V. P. Zhdanov, *ibid.* **111**, 63.
[94]V. P. Zhdanov, *ibid.* L662.
[95]V. P. Zhdanov, *ibid.* **133**, 469 (1983).
[96]V. P. Zhdanov, *ibid.* **171**, L461 (1986).
[97]V. P. Zhdanov, J. Chem. Soc. Faraday Trans. Ser. 2 **82**, 149 (1986).
[98]V. P. Zhdanov, Poverkhnost', No. 3, 20 (1985).
[99]Yu. K. Tovbin and V. K. Fedyanin, Kinet. Kataliz. **19**, 989, 1202 (1978); **20**, 1226 (1979); Fiz. Tverd. Tela (Leningrad) **22**, 1599 (1980) [Sov. Phys. Solid State **22**, 934 (1980)].
[100]S. Sundaresan and K. R. Kaza, Surf. Sci. **160**, 103 (1985); Chem. Ing. Commun. **32**, 333 (1985); **35**, 1.
[101]V. N. Ageev, Poverkhnost', No. 3, 5 (1984).
[102]P. Kisliuk, J. Phys. Chem. Sol. **3**, 95 (1957); **5**, 78 (1958).
[103]C. Kohrt and R. Gomer, J. Chem. Phys. **52**, 3283 (1970); Surf. Sci. **40**, 71 (1973).
[104]R. Gomer, Solid State Phys. **30**, 93 (1975).
[105]D. A. King, Surf. Sci. **40**, 71 (1973).
[106]R. Gort and L. D. Schmidt, *ibid.* **76**, 559 (1978).
[107]K. Schonhammer, *ibid.* **83**, L633 (1979).
[108]K. Christmann, O. Schober, and G. Ertl, J. Chem. Phys. **60**, 4719 (1974).
[109]H. Phnür, P. Feulner, H. A. Engelgardt, and D. Menzel, Chem. Phys. Lett. **59**, 481 (1978).
[110]H. Phnür, P. Feulner, and D. Menzel, J. Chem. Phys. **79**, 4613 (1983); Surf. Sci. **126**, 374 (1983).
[111]J. L. Taylor and W. H. Weinberg, *ibid.* **78**, 259 (1978).
[112]J. L. Taylor, D. E. Ibbotson, and W. H. Weinberg, J. Chem. Phys. **69**, 4298 (1978).
[113]H. Ibach, W. Erley, and H. Wagner, Surf. Sci. **92**, 29 (1980).
[114]C. T. Campbell, G. Ertl, and J. Segner, *ibid.* **115**, 309 (1982).
[115]M. V. Loginov, M. A. Mittsev, and A. M. Mukhuchev, Fiz. Tverd. Tela (Leningrad) **22**, 3299 (1980) [Sov. Phys. Solid State **22**, 1931 (1980)].
[116]E. Sommer and H. J. Kreuzer, Surf. Sci. **119**, L331 (1982).
[117]R. A. Redhead, Vacuum **12**, 203 (1962).
[118]L. D. Schmidt, Catal. Rev. **9**, 115 (1974).
[119]Y. Tokoro, T. Uchijima, and Y. Yoneda, J. Catal. **56**, 110 (1979).
[120]J. M. Soler and N. Garsia, Surf. Sci. **124**, 563 (1983).
[121]P. Forzatti, M. Borghesi, I. Pasqun, and E. Tronconi, *ibid.* **137**, 595 (1984).
[122]V. P. Zhdanov and Yu. N. Mordvintsev, Poverkhnost]', No. 9, 45 (1986).
[123]V. P. Zhdanov, Poverkhnost', No. 10, 23 (1984).
[124]M. Alnot and A. Cassuto, Surf. Sci. **112**, 325 (1981).
[125]R. G. Jones and D. L. Perry, *ibid.* **82**, 540 (1979).
[126]V. P. Zhdanov, *ibid.* **123**, 106 (1982).
[127]V. P. Zhdanov, *ibid.* **137**, 515 (1984).
[128]V. P. Zhdanov, *ibid.* **169**, 1 (1986).
[129]M. Bowker, *ibid.* **100**, L472 (1980).
[130]M. Alnot, J. Fusy, and A. Cassuto, *ibid.* **72**, 467 (1978).
[131]B. Hellsing and A. Malo, *ibid.* **144**, 336 (1984).
[132]R. Ducros, M. Alnot, J. J. Ehrhardt, M. Housley *et al.*, *ibid.* **94**, 154 (1980).
[133]J. B. Benziger, J. Chem. Soc. Faraday Trans. Ser. 1 **76**, 49 (1980).
[134]J. B. Benziger and G. R. Schoots, J. Phys. Chem. **88**, 4439 (1984).
[135]S. Yu. Surovtsev and Yu. K. Tovbin, Poverkhnost', No. 5, 22 (1985).
[136]V. P. Zhdanov, Surf. Sci. **148**, L691 (1984).
[137]V. P. Zhdanov, Poverkhnost', No. 1, 14 (1986).
[138]V. A. Kaminskiĭ, B. N. Okunev, and A. A. Ovchinnikov, Dokl. Akad. Nauk SSSR **251**, 636 (1980).
[139]S. Prager and H. L. Frisch, J. Chem. Phys. **72**, 2941 (1980).

[140]R. I. Cukier, *ibid.* **79**, 2430 (1983).
[141]G. Ehrlich and K. Stolt, Ann. Rev. Phys. Chem. **131**, 603 (1980).
[142]R. Gomer, Vacuum **33**, 537 (1983).
[143]R. Butz and H. Wagner, Surf. Sci. **63**, 448 (1977).
[144]R. DiFoggio and R. Gomer, Phys. Rev. B **25**, 3490 (1982).
[145]S. C.Wang and R. Gomer, J. Chem. Phys. **83**, 4193 (1985).
[146]M. Bowker and D. A. King, Surf. Sci. **71**, 583 (1978).
[147]M. Bowker and D. A. King, *ibid.* **72**, 208.
[148]H. Asada and M. Masuda, *ibid.* **99**, L429 (1980).
[149]D. A. Reed and G. Ehrlich, *ibid.* **102**, 588 (1981); 105, 603.
[150]G. E. Murch, Phil. Mag. A **43**, 871 (1981).
[151]W. Zwerger, Z. Phys. K1. B **42**, 333 (1981).
[152]G. Mazenko, J. R. Banavar, and R. Gomer, Surf. Sci. **107**, 459 (1981).
[153]A. Sadiq and K. Binder, *ibid.* **128**, 350 (1983).
[154]D. R. Bowman, *ibid.* **130**, 348.
[155]E. Oguz, *ibid.* **134**, 777.
[156]M. Tringides and R. Gomer, *ibid.* **145**, 121 (1984); **155**, 254 (1985).
[157]V. P. Zhdanov, *ibid.* **149**, L13.
[158]A. A. Tarasenko and A. A. Chumakh, Poverkhnost', No. 2, 35 (1983).
[159]A. A. Tarasenko, Poverkhnost', No. 5, 29 (1985).
[160]I. Yokota, J. Phys. Soc. Jpn. **21**, 420 (1966).
[161]A. H. Smith, R. A. Barker, and P. J. Estrup, Surf. Sci. **136**, 327 (1984).
[162]Y. Inaoka and A. Yoshimoria, *ibid.* **149**, 241 (1985).
[163]V. P. Zhdanov, *ibid.* **165**, L31 (1986).

Translated by M. E. Alferieff